Université du Québec
à Rimouski

DISTRIBUTION SPATIALE ET TEMPORELLE DES HYDROCARBURES AROMATIQUES POLYCYCLIQUES DANS LES SÉDIMENTS DE L'ARCHIPEL ARCTIQUE CANADIEN

Mémoire présenté

dans le cadre du programme de maîtrise en Océanographie

en vue de l'obtention du grade de maître ès sciences

PAR

© Anne Corminboeuf

9 avril 2021

Composition du jury :

Zhe Lu, président du jury, ISMER-UQAR

Jean-Carlos Montero-Serrano, directeur de recherche, ISMER-UQAR

Richard St-Louis, codirecteur de recherche, UQAR

Yves Gélinas, examinateur externe, Concordia University

Dépôt initial le 16 décembre 2020 Dépôt final le 9 avril 2021

[The Arctic] had evolved into a rich, conflicted metaphor of romance and heroism – a symbol of the conquest of man over nature, seat of the Romantic ideal. It was the zone of the marvellous, the unexpected, the fantastical.

Franklin's Lost Ship: The Historic Discovery of the HMS Erebus – John Geiger and Alanna Mitchell

REMERCIEMENTS

Je remercie sincèrement mon directeur de recherche, Jean-Carlos Montero-Serrano, pour la confiance dont il m'a fait preuve tout au long de ces deux années et surtout pour toute l'indépendance accordée. Je suis aussi reconnaissante de toutes les chances incroyables que j'ai eues pour les sorties terrain et les congrès. Je remercie également mon co-directeur de recherche, Richard St-Louis, dont le calme, l'optimisme et la bonne humeur ont toujours fait du bien. Je crois sincèrement avoir eu la meilleure équipe! Aussi, un chaleureux merci va aux membres du jury, M. Yves Gélinas et M. Zhe Lu, qui m'ont accordé de leur temps malgré leurs horaires chargés et chamboulés en cette charmante pandémie.

Des remerciements chaleureux vont aussi à Jade Brossard et à Maria-Emilia Rodriguez-Cuicas pour la complicité lors de nos longues heures de routes vers les congrès et pour les moments inoubliables passés sur l'Amundsen. Merci aussi à Joshua Evans, sans qui la mission 2019 aurait été affreusement longue et qui complétait à merveille la Mustang Gang!

Finalement, un merci tout spécial aux commandants Claude Lafrance et Jean-Luc Dugal ainsi qu'à l'équipage de l'Amundsen, l'équipe B tout particulièrement. Vous occupez une petite place spéciale dans mon cœur et mes souvenirs. Mes aventures nordiques n'auraient pas été aussi mémorables sans vous !

AVANT-PROPOS

Ce mémoire de maîtrise est présenté en trois parties : une introduction générale rédigée en français, un chapitre principal rédigé en anglais sous la forme d'un article scientifique en prévision d'être soumis pour publication à la revue internationale « *Marine Pollution Bulletin* » et une brève conclusion générale rédigée en français.

L'article présenté dans ce mémoire de maîtrise a été rédigé par moi-même avec la supervision des professeurs Jean-Carlos Montero-Serrano de l'UQAR-ISMER et Richard St-Louis de l'UQAR et il se présente ainsi: Corminboeuf, A., Montero-Serrano, J.-C., St-Louis, R. *Spatial and temporal distributions of polycyclic aromatic hydrocarbons in sediments from the Canadian Arctic Archipelago.* En tant que première autrice, ma contribution à ce travail fut la réalisation des extractions par ASE et des analyses par GC-MS des HAPs, le traitement des données, la création des figures et des graphiques et la rédaction de l'article. Jean-Carlos Montero-Serrano et Richard St-Louis ont fourni l'idée originale, l'implémentation du développement de la méthode, la formation nécessaire pour réaliser les analyses de données et les manipulations au laboratoire. Ils ont également contribué à la rédaction et à la révision de l'article. Des remerciements vont à Steeven Ouellet et Amy McMackin pour l'aide lors de l'utilisation du GC-MS et de son logiciel de traitement. Les données de ^{210}Pb utilisées dans l'article sont tirées du mémoire de maitrise de Sarah Letaïef : Letaïef, S. (2019). *Les processus sédimentaires durant le Petit âge glaciaire et l'actuel dans l'archipel arctique canadien*. Mémoire. Rimouski, Université du Québec à Rimouski, Institut des sciences de la mer de Rimouski (ISMER), 96 p. (http://semaphore.uqar.ca/id/eprint/1500/). Finalement, la qualité de l'anglais a été révisée par le groupe American Journal Experts.

Autres réalisations

En plus du travail au laboratoire, j'ai eu la chance de présenter mon projet de maîtrise et les résultats à plusieurs congrès nationaux et internationaux : Réunion scientifique annuelle de Québec-Océan (Rivière-du-Loup, 2018), Réunion scientifique annuelle d'ArcticNet (Ottawa, 2018 et Halifax, 2019), Congrès des étudiant-e-s du GÉOTOP (Orford, 2019), Réunion annuelle d'ArcTrain (Rimouski, 2019), 40th Annual North American Meeting of the Society of Environmental Toxicology and Chemistry (Toronto, 2019) et EGU General Assembly (Vienne, 2020, mais converti en congrès en ligne à cause de la pandémie de COVID-19).

J'ai aussi eu la chance de participer à trois missions d'échantillonnage dans l'Arctique canadien à bord du *NGCC Amundsen* (2017, 2018 et 2019) et à deux missions d'échantillonnage dans l'estuaire et le golfe du St-Laurent à bord du *NGCC Amundsen* (2020) et du *N/R Coriolis II* (2020).

Fig. 1. Photos à bord du *NGCC Amundsen* lors de la mission à l'été 2019 dans l'archipel Arctique canadien

RÉSUMÉ

Les concentrations de 23 hydrocarbures aromatiques polycycliques (HAPs) ont été déterminées dans 113 échantillons de sédiments marins de surface, 13 échantillons de sédiments terrestres et 80 sous-échantillons issus de 8 carottiers à boîte provenant de l'archipel arctique canadien (AAC) : mer de Beaufort; pente et plateau du Mackenzie; ouest de l'Île de Banks; détroit de M'Clure; golfes d'Amundsen, du Couronnement et de la Reine Maud; détroit de Victoria; Passage de M'Clintock; détroit de Barrow; passages de Wellington et de Peel; golfe de Boothia; détroit de Furry et Hecla; bassin de Foxe; détroits de Lancastre et de Jones; baie de Frobisher; canyon de Disko; détroits de Smith et de Nares, bassins de Kane et de Hall; passages de Kennedy et de Robertson. Les HAPs ont été extraits par une extraction accélérée par solvant (ASE) et quantifiés par chromatographie gazeuse couplée à un spectromètre de masse (GC-MS). Pour tout l'archipel, la somme des concentrations dans les sédiments marins de surface des 16 HAPs listés prioritaires par l'Agence de Protection de l'Environnement des États-Unis varie entre 7,8 et 247,7 ng g^{-1}(masse sèche) avec une valeur moyenne de 56,8 ng g^{-1}. Ces valeurs sont comparables à celles d'autres régions arctiques peu anthropisées (p. ex., la mer de Kara et la mer de Barents). Les apports en HAPs dans les sédiments au cours du dernier siècle sont restés constants et les concentrations se maintiennent dans les valeurs obtenues pour les sédiments de surface. L'utilisation des ratios diagnostiques du fluoranthène/(fluoranthène + pyrène) ainsi que du benz[a]anthracène/(benz[a]anthracène + pyrène) a permis de déterminer que les HAPs de l'AAC sont principalement d'origine pétrogénique naturelle, mais que certaines régions enregistrent aussi des HAPs d'origine pyrogénique. Les tendances temporelles n'indiquent pas de changement majeur dans le temps et indiquent également des apports principalement pétrogéniques. Certains résultats laissent croire à une influence grandissante des apports par les feux de forêt dont leur nombre et leur intensité augmentent dans le nord du Canada depuis les dernières décennies. En somme, l'AAC présente de faibles concentrations en HAPs, lesquels sont majoritairement d'origine naturelle.

Mots clés : Archipel arctique canadien, sédiments, hydrocarbures aromatiques polycycliques, ligne de base, pollution, holocène tardif.

ABSTRACT

The concentrations of 23 polycyclic aromatic hydrocarbons (PAHs) were calculated for 113 surficial marine sediments samples, 13 terrestrial sediment samples and 80 subsampled sediment samples from 8 pushcores from all the Canadian Arctic Archipelago (CAA): Beaufort Sea; Mackenzie slope and shelf; western Banks Island; M'Clure strait; Amundsen, Coronation and Queen Maud Gulfs; Victoria Strait; M'Clintock Channel; Barrow Strait; Wellington Channel; Peel Sound; Gulf of Boothia; Furry and Hecla Strait; Foxe Basin; Lancaster and Jones Sounds; Frobisher Bay; Disko Fan, Smith and Nares Straits; Kane and Hall Basins; Kennedy and Robertson channels. PAHs were extracted with an accelerated solvent extraction (ASE) and quantified with gas chromatography coupled to mass spectrometry (GC-MS). The sums of the concentrations of the 16 priority PAHs listed by the Environmental Protection Agency of the United States (US EPA) in surficial sediments ranged from 7.8 to 247.7 ng g^{-1} (dry weight basis) with a mean value of 56.8 ng g^{-1}. Those values are similar to those for other Arctic regions (e.g., Kara Sea and Barents Sea) with little anthropogenic influence. PAHs inputs to the sediments during the last century remained constant and stayed within the results obtained for surficial sediments. Diagnostic ratios of fluoranthene/(fluoranthene + pyrene) and benz[a]anthracene/(benz[a]anthracene + pyrene indicated that PAHs from the CAA are mainly from natural petrogenic sources, but some regions also record pyrogenic sources. Temporal trends do not indicate major source shifts and point mainly to petrogenic inputs. Some results tend to point a growing contribution to PAHs signature from forest fire events from northern Canada, those becoming more intense over the last decades. Globally, sediments from the CAA have low PAHs concentrations that are mainly natural.

Keywords: Canadian Arctic Archipelago, sediments, polycyclic aromatic hydrocarbons, baseline, pollution, Late Holocene.

TABLE DES MATIÈRES

LISTE DES TABLEAUX

LISTE DES FIGURES

LISTE DES ABRÉVIATIONS, DES SIGLES ET DES ACRONYMES

UQAR	Université du Québec à Rimouski
ISMER	Institut des sciences de la mer
HAPs	Hydrocarbures aromatiques polycycliques
PAHs	Polycyclic aromatic hydrocarbons
AAC	Archipel arctique canadien
CAA	Canadian Arctic Archipelago
US EPA	United States Environmental Protection Agency
AEE	Agence européenne de l'environnement
ADN	Acide désoxyribonucléique
CIRC	Centre international de recherche sur le cancer
ASE	Accelerated solvent extraction
GC-MS	Gas chromatograph coupled to a mass spectrometer
HPLC	High-performance liquid chromatography
Fla	Fluorantène/Fluoranthene
Pyr	Pyrène/Pyrene
B(a)A	Benz(a)anthracène/Benz(a)anthracene
Chr	Chrysène/Chrysene
K_{oa}	Indice octanol-air

Log K_{ow}	Logarithme de l'indice octanol-eau
Σ_{16}PAHs	Somme des 16 HAPs prioritaires de l'EPA
LMW	Low molecular weight
MMW	Medium molecular weight
HMW	High molecular weight
ERL	Effects range-low
EMR	Effects range-median

INTRODUCTION GÉNÉRALE

Les changements qui s'opèrent en Arctique

Depuis une quarantaine d'années, l'Arctique enregistre des changements majeurs, dont une diminution notable de son couvert de glace en termes d'épaisseur et de volume (Comiso *et al.*, 2008). En effet, depuis 1979, la couverture de glace mensuelle en septembre a diminué d'environ 13% par décennie (Scott et Hansen, 2016; Walsh *et al.*, 2017; National Snow and Ice Data Center, 2020). L'année 2012 a marqué un minimum historique de la plus faible extension en septembre, avec une étendue de $3{,}41 \times 10^6$ km^2 (Scott et Hansen, 2016). Ainsi, au cours des années 2030, les routes maritimes arctiques comme le Passage du Nord-Ouest, le Passage du Nord-Est et la Route Transpolaire seront soit majoritairement libres de glace ou partiellement couvertes de glace (de 40 à 60%) durant l'été (Askenov *et al.*, 2017). Le Passage du Nord-Ouest, une voie maritime située dans l'archipel arctique canadien (AAC), est alors appelé à s'imposer comme voie de navigation et de commerce international. En effet, il représente une alternative plus courte qu'emprunter le canal de Panama ou de Suez ou que de contourner les caps de Bonne-Espérance ou d'Horn afin de relier l'Asie et l'Europe (Lasserre *et al.*, 2010; Askenov *et al.*, 2017). L'utilisation des voies maritimes arctiques permettrait alors de réduire jusqu'à 40% les distances parcourues en mer tout en réduisant de façon conséquente l'utilisation de carburant et les émissions de CO_2 qui y sont reliées (Schøyen et Bråthen, 2011). La diminution de la couverture de glace et la circulation maritime ouvrent également la voie à des explorations et des exploitations minières ou pétrolières : la présence de ces ressources est attestée depuis longtemps, mais la difficulté d'accès au territoire avait mis le frein à une exploitation économiquement viable (AMAP, 2010; Simonet, 2016). Plus précisément, des réserves de pétrole et de gaz sont attestées dans l'ouest de l'AAC (secteurs du fleuve Mackenzie et de la mer de Beaufort; Thomas, 1979; Janicki, 2001; Yunker *et al.*, 2002a; Klungsøyr *et al.*, 2010) ainsi que dans l'est de l'AAC (secteurs de l'est de l'île de Baffin et de Scott Inlet; Levy, 1978). L'Institut d'études géologiques des États-Unis a estimé que les provinces géologiques des bassins intérieurs du Canada (ouest de l'AAC), du Bassin de Sverdrup (nord de l'AAC) ainsi que celles de l'ouest

groenlandaise/est canadienne renfermaient respectivement près de 90 millions, 2 500 millions et 17 000 millions de barils de pétrole et de gaz (Bird *et al.*, 2008). Déjà, dans les années 1960, 240 puits de forage ont été réalisés dans l'ouest de l'AAC, dont 83 se situaient au large de la mer de Beaufort (Klungsøyr *et al.*, 2010). Finalement, depuis les années 1990, 168 puits ont été forés sur le territoire arctique canadien (Klungsøyr *et al.*, 2010).

Une circulation maritime accrue et une augmentation des activités anthropiques en Arctique ne sont pas sans conséquences : ces activités génèrent et relâchent plusieurs composés dans l'environnement, dont des hydrocarbures aromatiques polycycliques (HAPs) (Lima *et al.*, 2005). Ces composés constituent un vaste groupe de contaminants organiques dont la structure chimique de base présente au moins deux benzènes (C_6H_6) fusionnés en plusieurs conformations possibles (Fig. 2) et tous caractérisés par de faibles solubilités dans l'eau et de faibles pressions de vapeur (Haritash et Kaushik, 2009; AMAP, 2017).

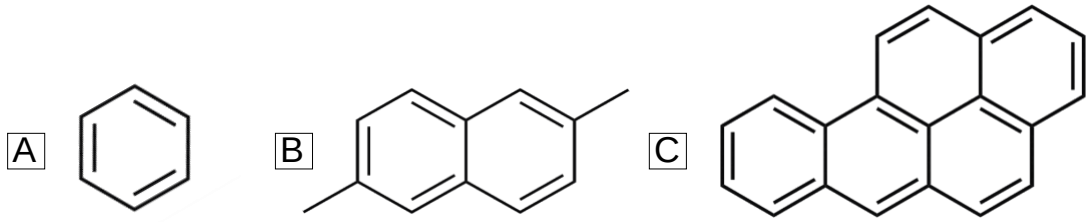

Fig. 2. (A) Structure et formule chimique de l'unité de base des HAPs, le benzène (B) du 2,6-diméthylnaphtalène et (C) du benzo(a)pyrène

Les sources des HAPs

Les HAPs peuvent être d'origine pétrogénique (Fig. 3), c'est-à-dire qu'ils sont issus de pertes par volatilisation des réserves pétrologiques naturelles, de déversements accidentels de produits pétroliers ou encore de l'érosion des roches continentales (Lima *et al.*, 2005; Wang *et al.*, 2007). Les HAPs pyrogéniques (Fig. 3) sont quant à eux produits lors d'une combustion incomplète de matériel carboné, qu'elle soit naturelle (p. ex., feux de forêt et éruptions volcaniques) ou anthropique (p. ex., combustion d'essence, de mazout, de diésel et de charbon, et émanations des industries comme les cimenteries ou les alumineries) (Chen *et al.*, 2018; Yu *et al.*, 2019). Les HAPs de sources pyrogéniques sont d'ailleurs les plus

présents dans l'environnement (Lima *et al.,* 2005). Finalement, les HAPs peuvent avoir une origine biogénique récente, c'est-à-dire qu'ils sont naturellement générés lors de processus biologiques, mais leur impact à large échelle est généralement considéré négligeable (Laflamme et Hites, 1978; Lima *et al.,* 2005, Klungsøyr *et al.,* 2010). Plusieurs centaines de HAPs peuvent être retrouvés dans l'environnement, mais 16 d'entre eux sont principalement étudiés parce qu'ils sont classés, depuis 1976, comme « polluants environnementaux prioritaires » par l'Agence de Protection de l'Environnement des États-Unis (US EPA) et l'Agence Européenne de l'environnement (AEE) (Keith, 2014; Pampanin et Sydnes, 2017; Roslund et *al.,* 2018). Le Canada les a également inscrits comme groupe de contaminants prioritaires (Meek *et al.,* 1994). Ces 16 HAPs sont majoritairement produits par une combustion d'essence et présentent une certaine toxicité et occurrence dans le temps et l'espace (AMAP, 2017).

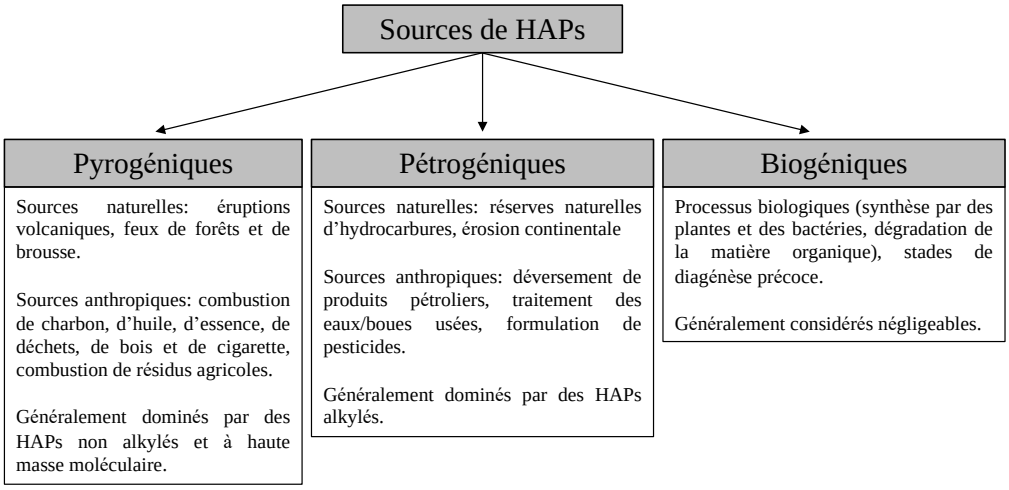

Fig. 3. Résumé des sources de HAPs (adapté de Klungsøyr *et al.,* 2010; Tobiszewski et Namieśnik, 2012; Mojiri *et al.,* 2019)

En 2007, les émissions mondiales de HAPs ont été estimées à 504 000 tonnes et le principal secteur d'émission était la combustion de biomasse (p. ex., feux de forêt et de cultures), pour environ 60,5 % des émissions totales (Shen *et al.,* 2013). Les véhicules motorisés ont contribué pour environ 12,8 % de ces émissions tandis que la déforestation et

les incendies ont compté pour environ 11,2%, la Chine et l'Inde étant les principaux pays émetteurs (Shen *et al.,* 2013). Les tendances mondiales de 1995 à 2008 montrent une diminution des émissions de HAPs de 592 000 tonnes à 499 000 tonnes grâce, entre autres, à des technologies de diminution des émissions et à une meilleure combustion des véhicules à moteur (Shen *et al.,* 2011; Shen *et al.,* 2013). En 2007, les émissions des 16 HAPs prioritaires de l'US EPA par les pays circumpolaires et avoisinant s'élevaient à 150 000 tonnes, soit 30% des émissions mondiales (Shen *et al.,* 2013). La Russie et les États-Unis arrivaient en tête des pays circumpolaires émetteurs avec les véhicules à moteur et les feux de forêts comme principales sources (Shen *et al.,* 2013). À long terme, l'étude de Shen et collaborateurs prévoit une baisse comprise entre 46 et 71% des émissions d'ici 2030. Malgré ces diminutions globales, les concentrations de HAPs dans l'atmosphère en Arctique des 20 dernières années ne montrent pas de réductions significatives, possiblement à cause des changements climatiques pouvant augmenter leur volatilisation et donc leur transport atmosphérique (Yu *et al.,* 2019). Ainsi, bien que plusieurs études prévoient des baisses des émissions mondiales des HAPs, il convient d'établir l'état actuel de la situation en Arctique afin de documenter la diminution anticipée.

Le devenir des HAPs dans l'environnement

Les HAPs d'origine pyrogénique sont principalement émis vers le compartiment atmosphérique et se retrouvent sous forme gazeuse ou liés aux particules comme les suies, les poussières minérales et les sels (Lima *et al.,* 2005; Tobiszewski et Namieśnik, 2012). Ce sont des composés semi-volatils qui peuvent alors voyager selon les vents d'une façon limitée, mais pouvant subir plusieurs cycles de volatilisation-déposition leur permettant d'effectuer du transport atmosphérique sur longue distance (Lima *et al.,* 2005; Tobiszewski et Namieśnik, 2012; Pampanin et Sydnes, 2017; AMAP, 2017; Chen *et al.,* 2018; Balmer *et al.,* 2019). Après une déposition sèche ou humide sur les sols, ils tendent à rester en place à cause de leur indice octanol-air (K_{oa}) élevé (Wang *et al.,* 2007) ou à s'infiltrer pour rejoindre le système aquatique (Klungsøyr *et al.,* 2010). S'ils sont déposés à la surface de l'eau, leur

nature hydrophobe (log K_{ow} compris entre 3,37 et 7) les fera se lier aux particules en suspension (Neff et Burns, 1996; Chen *et al.*, 2018; Zhao *et al.*, 2016). Les HAPs pétrogéniques, quant à eux, sont principalement émis vers le compartiment aquatique (Tobiszewski et Namieśnik, 2012). Ainsi, tous les HAPs devront passer par le compartiment aquatique et subir certains processus sédimentaires avant de se retrouver naturellement accumulés dans les sédiments à cause de leur affinité pour le compartiment organique (Chiou *et al.*, 1998; Gschwend and Hites, 1981; Stark *et al.*, 2003, Wang *et al.*, 2007).

Plusieurs processus naturels influencent le transport sédimentaire en Arctique. Les sédiments modernes du fond de l'AAC proviennent des décharges de diverses rivières (p. ex., les rivières Coppermine, Back, Ellice, Cunningham; Alkire *et al.*, 2017) et de l'érosion glaciaire des masses terrestres environnantes par divers processus sédimentaires (p. ex., les coulées de débris glaciogéniques, les panaches d'eau de fonte et les courants de turbidité) qui sont dominants dans les environnements glaciaires (Hiscott *et al.*, 1989; Ó Cofaigh *et al.*, 2003; Dowdeswell *et al.*, 2015). De plus, la glace de mer, les glaciers et les icebergs contribuent à emprisonner et à déplacer sur de très longues distances d'importantes quantités de sédiments (Stein, 2008). Les canyons sous-marins, et les transports de masse qui les parcourent régulièrement, permettent également de faire voyager des sédiments terrigènes vers les grands fonds marins (Harris, 2012; Lai *et al*., 2016). En fonction de leur taille et des courants, les particules vont éventuellement chuter et les HAPs pourront alors s'accumuler dans les sédiments, où ils seront stabilisés et ne subiront pratiquement plus de modifications (Fig. 4; Page *et al.*, 1999).

En milieu naturel, les HAPs ne sont pas facilement dégradés, ce qui leur procure un caractère semi-persistant (Pelletier *et al.*, 2008; Haritash et Kaushik, 2009). Leur dégradation peut être chimique (photooxydation), mais la dégradation biologique par les bactéries, les algues et les champignons est reconnue comme le principal mécanisme de dégradation (Haritash et Kaushik, 2009; Roslund *et al*., 2018). Les HAPs peuvent pénétrer dans les macro-organismes via leur diète et tendent à s'accumuler ensuite dans les tissus riches en lipides, comme le foie (Meador *et al.*, 1995). Les invertébrés comme les moules bleues sont

susceptibles d'accumuler d'importantes quantités de HAPs s'ils se développent dans des sites hautement pollués (Klungsøyr *et al.*, 2010). Par contre, la plupart des vertébrés, comme les poissons, les oiseaux et les mammifères, peuvent facilement les métaboliser (Xue et Warshawsky, 2005; Haritash et Kaushik, 2009). Le foie de morues arctiques (*Boreogadus saida*) pêchées au large de la mer de Beaufort et de morues de l'atlantique (*Gadus morhua*) pêchées en Islande et en Norvège présentait de faibles niveaux de métabolites de HAPs vraisemblablement attribuables à des sources naturelles (Tomy *et al.*, 2014; Jörrundsdóttir *et al.*, 2014). Ainsi, les HAPs légers et moyens ne subissent généralement pas de biomagnification le long de la chaîne alimentaire et il se produit plutôt une dilution en fonction du niveau trophique (Wan *et al.*, 2007; De Laender *et al.*, 2011).

Les HAPs sont éliminés des organismes grâce à une biotransformation par le foie et sont ensuite excrétés sous forme de composés-parents et de métabolites via l'urine et la bile (Balk *et al.*, 1984, Meador *et al.*, 1995). Les enzymes de la phase 1 (cytochrome P4501A) produisent des métabolites de HAPs qui sont généralement hydroxylés, mais des phénols, des dihydrodiols, des quinones et des époxydes peuvent aussi être formés (Stein *et al.*, 1984; Payne *et al.*, 1987; Tuvikene *et al.*, 1996). Les époxydes et les dihydrodiols sont des métabolites réactifs qui peuvent se lier à l'ADN et produire des adduits (Neff, 1985; Van Schooten, 1991; Pampanin et Sydnes, 2017). Ces adduits constituent des dommages à l'ADN pouvant produire des mutations, elles-mêmes menant à des tumeurs et à des cancers (Van Schooten, 1991; Pampanin et Sydnes, 2017). Ainsi, la métabolisation des HAPs par les vertébrés est un évènement-clé qui active le caractère cancérogène de ces molécules (Van Schooten, 1991; Xue et Warshawsky, 2005). Pour l'instant, 7 HAPs sont classés comme « possiblement cancérogène » chez l'humain (groupe 2B) par le Centre International de Recherche sur le Cancer de l'Organisation Mondiale de la Santé (CIRC) (Tremblay *et al.*, 2000). Finalement, dans l'environnement, les HAPs sont toujours présents sous forme de mélange et leurs proportions dépendent en grande partie de leur processus de formation, rendant ainsi possible l'utilisation de ratio diagnostique établissant leur origine, comme ratio du fluoranthène sur la somme de fluoranthène et de pyrène : des valeurs inférieures à 0,4 sont associées à des sources pétrogéniques, des valeurs comprises entre 0,4 et 0,5 sont associées

à des sources pyrogéniques de combustibles fossiles et des valeurs supérieures à 0,5 sont associées à des sources pyrogéniques de biomasse (Tobiszewski et Namieśnik, 2012).

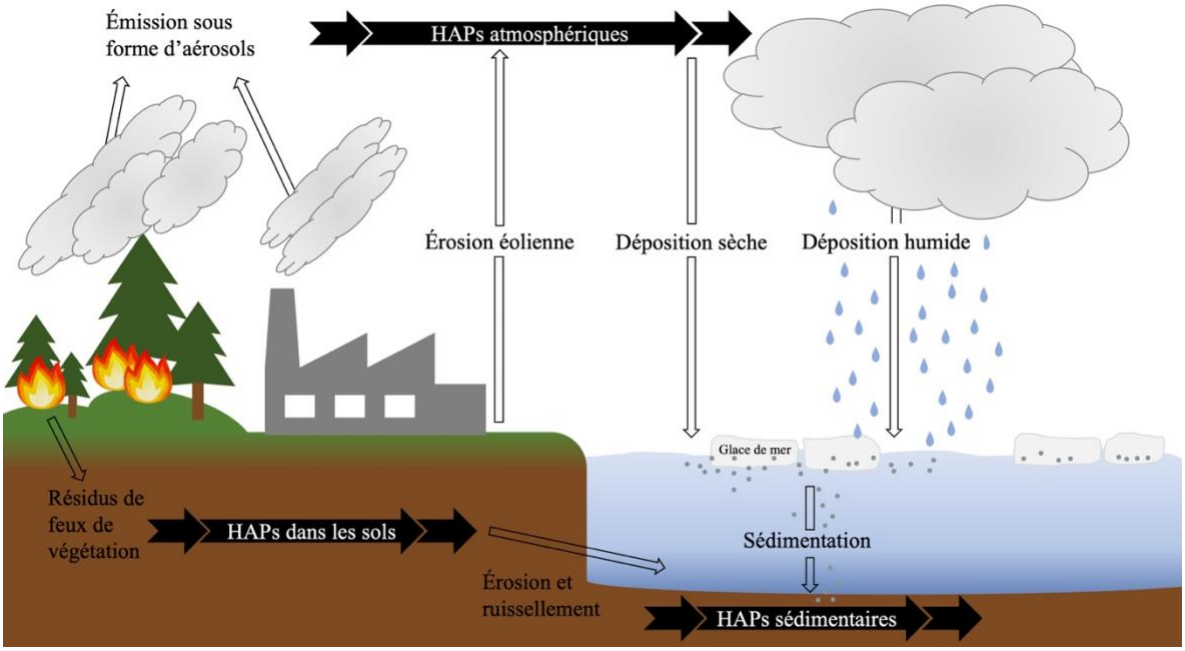

Fig. 4. Résumé du devenir des HAPs dans l'environnement (adapté de Doucette, 2006)

Le manque de connaissance sur le territoire et la pertinence de la recherche

Le territoire Arctique est vaste ; son accès restreint et son éloignement rendent difficile la réalisation d'études portant sur son ensemble. De plus, la vaste majorité des fonds marins et des plateaux continentaux restent méconnus en termes de composition chimique des sédiments (Stein, 2008). Précédemment, des études sur les concentrations récentes et passées en HAPs ont été effectuées sur des portions précises du territoire comme la mer de Beaufort (Yunker *et al.,* 1995, 2002a, 2002b) ou encore le nord de la Baie de Baffin (Foster *et al.,* 2015). À notre connaissance, aucune d'elle n'a dressé de portrait total de la distribution spatiale et temporelle des concentrations en HAPs dans les sédiments de l'archipel arctique canadien, incluant l'archipel central. Dans un contexte où l'Arctique subit de grands changements qui pourront mener à un accroissement des activités anthropiques (activités

maritimes, minières et exploration/exploitation pétrolière entre autres; Klungsøyr *et al.*, 2010, Askenov *et al.,* 2017), que ces activités sont sujettes à produire des HAPs et que ceux-ci peuvent s'accumuler dans les sédiments, il est alors primordial d'étudier en détails les sédiments afin d'obtenir un portrait global et actuel de leur distribution.

Objectifs de recherche

L'objectif principal de cette étude est de déterminer l'état actuel de la concentration et de la distribution des hydrocarbures aromatiques polycycliques dans les sédiments récents et dans les sédiments pré-industriels de l'archipel arctique canadien. Cet objectif global sera atteint grâce aux objectifs spécifiques suivant :

(1) Caractériser la distribution spatiale des concentrations en HAPs dans les sédiments marins récent et des sédiments terrestres provenant d'une grande partie de l'archipel arctique canadien;
(2) Déterminer les tendances temporelles des concentrations en HAPs à partir de carottiers à boîtes répartis dans l'AAC et datés au plomb 210 (Letaïef, 2019);
(3) Déterminer l'origine (pétrogénique ou pyrogénique) des HAPs par l'utilisation de ratios diagnostiques.

Les HAPs analysés sont les suivants: **naphtalène**, 1-méthylnaphtalène, 2-méthylnaphtalène, 2,6-diméthylnaphtalène, **acénaphtylène, acénaphtène**, 2,3,5-triméthylnaphtalène, **fluorène, phénanthrène, anthracène**, 1-méthylphénanthrène, 3,6-diméthylphénanthrène, **fluoranthène, pyrène**, 9,10-diméthylanthracène, **benz(a)anthracène, chrysène, benzo(b)fluoranthène, benzo(k)fluoranthène, benzo(a)pyrène, indéno(1,2,3-c,d)pyrène, dibenz(a,h,)anthracène et benzo(g,h,i)pérylène** (en **gras**, les 16 HAPs prioritaires de l'US EPA).

Afin de distinguer une source pétrogénique de pyrogénique, le ratio de fluoranthène sur la somme de fluoranthène et de pyrène (Fla/[Fla+Pyr]) et le ratio de benz(a)anthracène sur la

somme de benz(a)anthracène et de chrysène (BaA/[BaA+Chr]) seront utilisés (Yunker *et al.*, 2002b; Foster *et al.*, 2015).

SPATIAL AND TEMPORAL DISTRIBUTIONS OF POLYCYCLIC AROMATIC HYDROCARBONS IN SEDIMENTS FROM THE CANADIAN ARCTIC ARCHIPELAGO

Anne Corminboeuf [1,*], Jean-Carlos Montero-Serrano [1], Richard St-Louis [2]

[1] Institut des sciences de la mer de Rimouski (ISMER), Université du Québec à Rimouski, GEOTOP Research Center & Québec-Océan, 310 Allée des Ursulines, Rimouski, QC, G5L 3A1, Canada

[2] Université du Québec à Rimouski, 300 Allée des Ursulines, Rimouski, QC, G5L 3A1, Canada

* Corresponding author: A. Corminboeuf: annecorminboeuf@hotmail.com

1. INTRODUCTION

Within the context of climate change, the Arctic is undergoing major perturbations, and many studies have focused on sea ice conditions and navigability projections in the Arctic Ocean (Lasserre *et al.*, 2010; Askenov *et al.*, 2017). Because the summer sea ice extent is rapidly decreasing, leading to a seasonally ice-free Arctic Ocean, it has been speculated that maritime traffic could increase within the Canadian Arctic Archipelago (CAA); for example, the northwest passage could open to cargo transportation for a longer time period each year by the middle of the century (Lasserre *et al.*, 2010; Smith and Stephenson, 2013). This shipping route connecting Asia and Europe is shorter than the Suez Canal, the Panama Canal or the Cape of Good Hope (Lasserre *et al.*, 2010; Askenov *et al.*, 2017). Hence, maritime companies are interested in traveling through the Arctic since this would allow time and fuel savings and consequent cost reductions. However, maritime traffic and oil exploration within the Arctic could also increase the anthropogenic pressure and pollution load in Arctic ecosystems (Jörrundsdóttir, 2014).

Shipping-related fuel combustion and anthropogenic activities are local sources of polycyclic aromatic hydrocarbons (PAHs), which constitute a wide class of organic compounds consisting of more than one benzene ring (C_6H_6) fused in a variety of conformations (AMAP, 2017; Haritash and Kaushik, 2009). Hundreds of these compounds

are found in the environment, but since the mid 1970s, 16 PAHs have been listed as priority environmental pollutants by the Environmental Protection Agency of the United States (US EPA) and are therefore closely monitored (Keith *et al.,* 2014; Pampanin and Sydnes, 2017).

PAHs are introduced to the environment via natural or anthropogenic sources (Lima *et al.,* 2005; Foster *et al.,* 2015; Chen *et al*., 2018), and anthropogenic activities are major sources of the PAHs occurring in the biosphere (Yanik *et al.,* 2003; Morillo *et al.,* 2008). Seven PAHs have been classified as probably carcinogenic for humans by the International Agency for Research on Cancer (IARC) of the World Health Organization because of the reactivity of their metabolites (IARC, 1987). Inuit communities within the Arctic might be exposed to PAHs via the consumption of traditional foods, especially invertebrates such as mollusks (Rapinski *et al.,* 2018). However, the Arctic is a region where the seafloor composition is the least studied and understood. Indeed, the vast majority of the channels within the CAA and their adjoining continental shelves and slopes exhibit a substantial knowledge gap regarding sediment composition and associated contaminants (Stein, 2008). Moreover, studies have focused on specific areas of the Arctic (e.g., Beaufort Sea or Baffin Bay; Yunker *et al.,* 1995, 2002a, 2002b; Foster *et al.,* 2015) or sites near anthropogenic influences (Boitsov *et al.,* 2009a,b; Zaborska *et al.,* 2011). To our knowledge, no complete baseline information on the PAHs in recent sediments or historic tendencies of the PAH inputs to sediments are available within the CAA.

2. SOURCES OF PAHS AND THEIR ENVIRONMENTAL FATE WITHIN THE CAA

2.1 PAHs sources

Pyrogenic PAHs are produced during the incomplete combustion of organic matter, which includes forest and bush fires and fossil fuel and coal combustion (Chen *et al.,* 2018; Yu *et al.,* 2019). These PAHs are mainly emitted into the atmosphere and could occur either in the gaseous phase or bonded to the particulate phase (i.e., mineral dust and salt) (Tobiszewski and Namieśnik, 2012). Owing to their low vapor pressures, the majority of

these semivolatile compounds undergoes repeated cycles of volatilization-deposition, travel across long distances and eventually end up in waters, soils and sediments via atmospheric deposition (AMAP, 2017; Chen *et al.*, 2018; Balmer *et al.,* 2019). The PAHs produced at mid-latitudes could thus reach the Arctic, as shown by modeling studies (Wang *et al.,* 2010; Sofowote *et al*., 2011).

Petrogenic PAHs are hydrocarbons stemming from losses or seepages of oil and petroleum deposits, crude oil spills or rock weathering and are therefore naturally present in sediments and water bodies, and these PAHs are not of great concern because of their very low concentration (Lima *et al.,* 2005; Pampanin and Sydnes, 2017; Chen *et al.,* 2018). They are readily dispersed via water runoff, and since petrogenic PAHs are not directly emitted into the atmosphere, they are slightly influenced by long-range atmospheric transport (Pampanin and Sydnes, 2017).

2.2 Environmental fate

In the Arctic, PAHs stemming from distant sources may enter the marine environment via river discharge, but long-range atmospheric transport is believed to be a significant input process (Sofowote *et al.,* 2011; Yu *et al.,* 2019). Regarding the environmental fate of atmospheric PAHs, Lammel *et al*. (2009) showed via a modeling approach that between 0.5% and 12.8% of the total environmental burden of PAHs might be stored within Arctic ecosystems (i.e., air, soil, vegetation and ocean) depending on the chosen gas/particle partitioning scenario. In addition to the already existing natural PAHs in Arctic soils and sediments, atmospheric deposition of PAHs originating from remote sources, in addition to new local sources such as ship traffic and oil exploration/exploitation, are PAH sources in the CAA (Balmer *et al.,* 2019). PAHs are not easily degraded under natural conditions and are therefore slightly persistent (Pelletier *et al.,* 2008; Haritash and Kaushik, 2009). Photooxidation of PAHs is a chemical pathway of degradation, but biological degradation by bacteria, fungi and algae is accepted as the main process (Roslund *et al.,* 2018; Haritash and Kaushik, 2009; Balmer *et al.,* 2019). Because most vertebrates (e.g., fishes, birds and

mammals) readily metabolize PAHs, they do not tend to experience biomagnification through the food chain (Xue et Warshawsky, 2005; Haritash et Kaushik, 2009; AMAP, 2017). During their metabolism, the phase 1 enzymes produce various PAH-metabolites and some of them, such as the epoxides and the dihydrols, might cause DNA adducts leading to a carcinogenic and mutagenic potential (Stein *et al.*, 1984; Neff, 1985; Payne *et al.*, 1987; Van Schooten, 1991; Tuvikene *et al*., 1996; Pampanin et Sydnes, 2017). However, PAHs could accumulate in benthic species such as clams and mussels (Balmer *et al.* 2019), and these organisms are an important food source for northern communities (Jörrundsdóttir *et al.*, 2014; Rapinski *et al.* 2018). If deposited on land, PAHs could leach through soils or could be transported via water runoff and eventually reach aquatic ecosystems (Wang *et al.*, 2007; Klungsøyr *et al.*, 2010). They are poorly soluble in water because of their hydrophobicity and lipophilicity (Chen *et al.*, 2008; Zhao *et al.*, 2016). Consequently, PAHs exhibit a relatively high affinity for suspended and particulate matter and sediments, which is why the latter are considered the main sink of PAHs (Chen *et al.*, 2008).

Considering that PAHs are pollutants of interest that could be released by an increase in anthropogenic activities in the Arctic and that could accumulate in sediments and considering that the Arctic sediment PAH composition is not completely known, it is essential to determine the actual baseline. The aim of this study is to (1) characterize the spatial distribution patterns of the PAHs within the CAA modern sediments, (2) determine the temporal trends of the PAH concentration based on ^{210}Pb-dated box cores collected across the CAA, and (3) establish the origin of PAHs (i.e., petrogenic or pyrogenic) according to two diagnostic ratios: fluoranthene over the sum of fluoranthene and pyrene (Fla/[Fla+Pyr]) and benz(a)anthracene over the sum of benz(a)anthracene and chrysene (BaA/[BaA+Chr]).

3. MATERIALS AND METHODS

3.1 Study site

Since pyrogenic PAHs traveling via long-range atmospheric transport are deposited in soil or water and petrogenic PAHs mainly originate from rock weathering and oil reserves, they both occur in sediments, i.e., sediments are a sink for organic pollutants such as PAHs, and their affinity for fine and organic-rich sediments is well documented (Chiou *et al.*, 1998; Gschwend and Hites, 1981; Stark *et al.*, 2003). Letaïef (2019) reported that the sediments within the CAA ranged from clay (2 µm) to fine silt (4 to 8 µm). The total organic carbon (TOC) content is lower than 2% in most surface sediments retrieved from the CAA (e.g., Letaïef, 2019). More specifically, the Mackenzie Shelf and Delta and the Beaufort Sea/Canada Basin exhibit TOC values ranging from 0.5% to 1.9% (Yunker *et al.*, 2011; Letaïef, 2019). The Queen Maud Gulf and the M'Clintock Channel, central CAA, exhibit relatively low TOC contents, with values ranging from 0.2% to 0.5 % (Letaïef, 2019). Finally, the TOC content in Baffin Bay sediments ranges from 0.2% to 1.5% (Stein, 1991; Madaj, 2016). The CAA counts approximately 36500 islands and numerous waterways, straits, channels and sills formed by glacial action under past climate conditions (Melling *et al.*, 2002; Michel *et al.*, 2006). The recent sedimentary dynamics within the CAA are controlled by the sediment supply stemming from river discharge in the west and central CAA, whereas the east CAA is more influenced by sea ice and coastal erosion (Letaïef, 2019). Indeed, the Mackenzie River alone annually discharges approximately 420 km^3/yr of sediments onto the continental shelf of the Beaufort Sea and is therefore a major source of continental PAHs (Wagner *et al.*, 2011). Other small rivers exert a cumulative significant impact on the sediment load, such as the Coppermine River, the Ellice and Back Rivers and the Cunningham River, with a total contribution of approximately 110 km^3/yr (Alkire *et al.*, 2017). Once in the marine ecosystem, sediments are entrained throughout the archipelago by sea ice via suspension freezing and ice anchoring (Reimnitz *et al.*, 1993; Darby *et al.*, 2003, 2011; Stein, 2008). Coastal erosion by seasonal sea ice, glaciogenic debris flows, meltwater plumes, mass movements along submarine canyons and sea lifting are other dominant

sedimentary processes in glacial environments contributing to the dispersal of sediments across great distances within the CAA (Hiscott *et al.*, 1989; Ó Cofaigh *et al.*, 2003; Harris, 2012; Dowdeswell *et al.*, 2015; Lai *et al*., 2016). Processes involving sea ice are mostly active during the sea ice formation season, and sediments are discharged elsewhere during summer melting (Darby *et al*., 2011). All of these processes contribute to the dispersion of PAHs originating from distant sources within the CAA before they become trapped in marine sediments.

3.2 Material and reagents

All reagents were of analytical or high-performance liquid chromatography (HPLC) grade. Hexanes and dichloromethane were obtained from Anachemia, methanol was acquired from Millipore and 2-propanol was obtained from Fisher Chemicals. Nitric acid (HNO_3) and hydrochloric acid (HCl) were acquired from VWR Analytical. Silica gel (technical grade, 70-230 mesh) and copper powder (<425 µm) were obtained from Sigma-Aldrich. Diatomaceous earth (celite 566) was acquired from UCT Enviro-Clean. Standard reference material NIST-1944 was purchased from the National Institute of Standards and Technology (NIST). PAH Mix manufactured by AccuStandard was adopted for the generation of calibration curves, combined with an alkylated PAH homemade mix (2,6-dimethylnaphthalene and 9,10-dimethylanthracene were obtained from Sigma-Aldrich, while 2,3,5-trimethylnaphthalene, 1-methtylnaphthalene and 3,6-dimethylphenanthrene were acquired from Fisher Chemicals). Before analysis, every sample was spiked with deuterated 1-methylnaphthalene and benz(a)anthracene purchased from Sigma. A mixture of deuterated naphthalene (Sigma-Aldrich), anthracene (Cambridge Isotope Laboratories) and perylene (Sigma-Aldrich) was added as internal standards for quantification purposes. The targeted compounds in this study included 16 parent PAHs and 7 alkylated PAHs: naphthalene, 1-methylnaphthalene, 2-methylnaphthalene, 2,6-dimethylnaphthalene, acenaphthylene, acenaphthene, 2,3,5-trimethylnaphthalene, fluorene, phenanthrene, anthracene, 1-methylphenanthrene, 3,6-dimethylphenanthrene, fluoranthene, pyrene, 9,10-

dimethylanthracene, benz(a)anthracene, chrysene, benzo(b)fluoranthene, benzo(k)fluoranthene, benzo(a)pyrene, indeno(1,2,3-c,d)pyrene, dibenz(a,h)anthracene and benzo(g,h,i)perylene.

Silica gel was activated at 450°C for 2 h and stored in a desiccator. Copper powder, for sulfur removal from sediments, was activated as follows: in a Teflon tube, copper powder was covered with hydrochloric acid (HCl) 6N and shaken for 3 min. It was then rinsed with distilled water until a neutral pH was attained. The copper powder was then washed 3 times with both methanol and dichloromethane and was finally stored in a Teflon tube covered with dichloromethane.

3.3 Sediment samples and chronology

A total of 126 sediment samples was analyzed in this study: 113 marine surface sediment samples and 13 terrestrial sediment samples collected from glaciers (glacial till) and rivers (Fig. 5). Additionally, 8 push cores were subsampled to determine temporal trends (Fig. 5). All samples were retrieved from box cores collected between 2016 and 2019 across a large area covering the Canadian Beaufort Sea to Baffin Bay during the ArcticNet summer expeditions onboard the Canadian Coast Guard Ship (CCGS) icebreaker Amundsen. Samples were collected from glaciers and rivers using the ship helicopter as CCGS Amundsen traveled through the CAA. All marine coring sites were targeted using high-resolution seismic profiles, which indicated that Late Holocene sediment accumulation was not influenced by mass wasting events (Montero-Serrano *et al.*, 2016, 2017, 2018, 2019). Surface sediments (uppermost 0.5 to 1 cm) were collected with a spoon and stored in plastic bags (WhirlPack) at 4°C until further analysis. Push cores were collected by pushing a plexiglass tube (10-cm diameter) into sediments. The cores were stored at 4°C until further subsampling. Sediment subsamples were retrieved from the push cores from 0 to 10 cm at 1-cm intervals. Age-depth models of the box cores have been previously published in Letaïef (2019), and were constructed using ^{210}Pb measurements combined with the constant rate of supply (CRS) model (a constant rate of the ^{210}Pb supply; Appleby and Oldfield, 1983). The age is reported

as common era (CE) and before common era (BCE) hereafter. The sedimentation rates and ages at ~10 cm depth are provided in Table 1 and Fig. S1. Note that no dates are available for core AMD1902-05BC recovered in the Robeson Channel (Fig. 5). However, based on the sedimentation rate (4 cm ka^{-1}) determined for a well-dated neighboring core (HLY03-05GC; Jennings *et al.*, 2011), we inferred that the age at a core depth of ~10 cm is approximately 2.5 cal ka BP (550 BCE).

Table 1. Sedimentation rate and sediment age at ~10 cm of the push-cores used in this study

Core ID	**Sedimentation rate (cm ka^{-1})**	**Age (~10 cm of core depth)**
AMD1604-05BC	178	1956 CE
AMD1603-165BC	82	1894 CE
AMD1603-304BC	184	1962 CE
AMD1603-316BC	111	1926 CE
AMD1603-408BC	87	1901 CE
AMD1603-535BC	113	1928 CE
AMD1603-QMG4BC	164	1955 CE
AMD1902-05BC	4*	550 BCE

* Sedimentation rate inferred from Jennings *et al.* (2011).

All samples were sieved through a 150-µm Nitex® mesh using distilled water. The <150 µm sediment fraction was then stored in a 50-mL Falcon® tube successively rinsed with tap water and soap, distilled water, nitric acid (HNO_3) 5% (3 times), distilled water and 2-propanol (3 times). The sediment samples were then frozen at -80°C for at least 12 h and freeze dried. The samples were finally crushed using an agate mortar. Aliquots weighing 5 g of these homogenized sediment samples were used for PAH analysis.

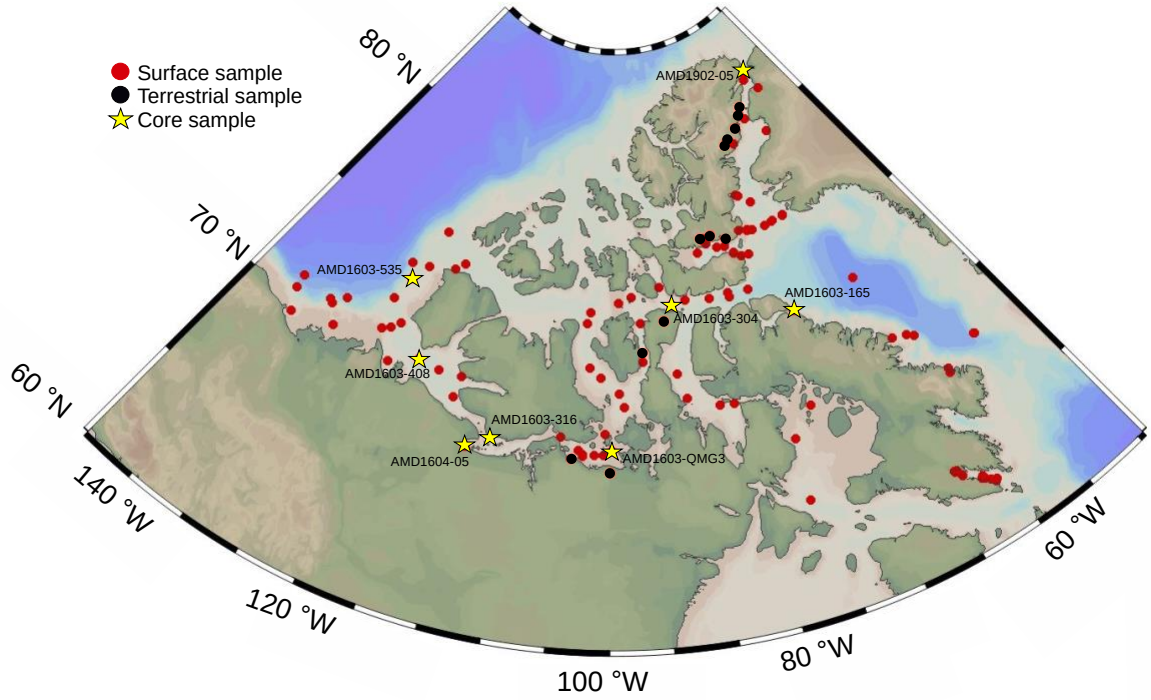

Fig. 5. Locations of the sediment samples collected from the Canadian Arctic Archipelago

3.4 Carbon analysis

Carbon analyses were performed on surface samples at the GEOTOP light stable isotope geochemistry laboratory (Montreal, Québec) using a Carlo-Erba NC 2500 elemental analyzer. For this, each freeze-dried and milled sediment sample was divided into two aliquots. A first aliquot of bulk sediment was used to determine the total carbon (TC) content. A second aliquot was acidified with 1 M HCl to remove carbonates, dried and milled. This carbonate-free aliquot was used to determine the total organic carbon (TOC) content. An empirical correction was applied to the TOC results (expressed in weight percent, wt. %) to account for changes in sample mass due to carbonate removal process (Hélie, 2009). Analytical precision and accuracy were determined by replicating analyses of samples and replicate analyses of in-house and international standards (low organic content soil, cyclohexanone-2,4-dinitrophenylhydrazone, atropine and acetanilide) and were better than ±0.02% (1σ).

3.5 PAHs extraction and analysis

PAH extraction was conducted via accelerated solvent extraction (ASE) following the method developed by Choi *et al.* (2014). Briefly, 22-mL stainless-steel extraction cells were loaded as follows, from bottom to top: cellulose filter, diatomaceous earth, activated silica gel (5 g), activated copper (5 g), freeze-dried sediment sample (5 g) and diatomaceous earth to the top (Fig. S2). A PAH spike (1-methylnaphthalene-d10 and benz(a)anthracene-d12) was directly added onto the sediment sample. The cells were maintained open and protected from dust contamination at room temperature for 2 h to acclimate. Blanks were prepared similar to the samples but with no sediments. To confirm the accuracy of the method, 0.5 g of standard reference material NIST-1944 was processed as a sample. One blank, one standard reference material sample and one duplicate were tested for every 12 samples.

The addition of activated silica gel and copper directly to the cell enabled one-step extraction and cleanup. The extraction was performed with a Dionex ASE 200 system (Thermo Co., Sunnyvale, CA, USA). The temperature and pressure were set to 100°C and 1700 psi, respectively. The flush volume and purge time were set at 60% and 100 s, respectively. The extraction was performed with a mixture of hexane and dichloromethane (at a ratio of 4:1 v/v) and two static cycles of 5 min. Extracts were collected in 60-mL clear collection vials (previously rinsed with tap water and soap, distilled water, hexane and dichloromethane (4:1 v/v) mixture and propanol). The extracts were then evaporated to approximately 5 mL with a rotating evaporator and then evaporated to exactly 0.5 mL with a nitrogen stream at room temperature. In regard to standard material NIST-1944, the extracts were evaporated to exactly 1.5 mL.

PAH analyses were performed via gas chromatography (GC, Agilent Technologies 6850 series II; Santa Clara, CA, USA) coupled with mass spectrometry (MS, Agilent Technologies 5975B VL MSD) using total ion count (TIC). The injection was performed with an Agilent Technologies Autosampler 6850. The capillary column used was an Rxi®-5 ms (30 m x 0.25-mm inner diameter (ID) x 0.25 µm ft, 5% diphenyl and 95% polysiloxane

from RESTEK). The oven temperature was set as follow: 50°C for 2 min, 15°C/min until 275°C, held for 2 min, 15°C/min until 325°C, held for 15 min, and a postrun of 2 min at 300°C. A sample volume of 1 µL was injected at a temperature of 250°C under splitless injection with helium as the carrier gas at a flow rate of 1 mL/min.

3.6 Quality control and quality assurance (QC/QA)

The procedural blanks did not reveal contamination. Hence, the results were not blank corrected. The spike recoveries were 73.7% ± 15.0% for 1-methynaphthalene-d10 and 83.5% ± 23.2% for benz(a)anthracene-d12. Some samples did not meet the generally accepted QC/QA recovery criteria of 70% to 103%. All samples were hence spike corrected. The efficiency of the method was confirmed with standard reference material NIST-1944. The mean recoveries obtained are compared in Table S1 to those obtained by Choi *et al.* (2014), who developed the ASE method applied in this study. The method detection limit (MDL) for each PAH was calculated as suggested by the US EPA (Oblinger Childress *et al.*, 1999). Briefly, 7 replicates of the second lowest calibration point were injected and analyzed. Hence, the MDL was determined as 3.143 times (Student's *t* value for 6 degrees of freedom and the 99% confidence level) the standard deviation of the measured concentration for each compound. The MDL ranged from 1.6 ng g^{-1} for benz(a)anthracene to 31.2 ng g^{-1} for acenaphthylene (Table S2).

3.7 Data processing

Prior to all multivariate analyses, the values below the detection limit (VBDLs) were imputed via multiplicative lognormal replacement with R package zCompositions (Palarea-Albaladejo and Martin-Fernandez, 2015). This method preserves the geometry of the compositional data while accounting for corresponding detection limit thresholds. However, variables with VBDLs greater than 30% [such as acenaphthylene, 2,3,5-trimethylnaphthalene, benz(a)anthracene, benzo(b)fluoranthene, benzo(k)fluoranthene,

benzo(a)pyrene, indeno(1,2,3-c,d)pyrene, dibenz(a,h)anthracene, and benzo(g,h,i)perylene] were omitted in the subsequent multivariate analyses (Palarea-Albaladejo and Martin-Fernandez, 2015). Next, a log-centered (clr) transform was applied to the data (Aitchison, 1990). This operation removed the statistical constraints on the compositional variables, such as the constant-unit sum, and enabled the valid application of classical (Euclidean) statistical methods to the compositional data (Aitchison, 1986, 1990; Montero-Serrano *et al.*, 2010). We applied fuzzy c-means (FCM) clustering analysis (Kaufman and Rousseeuw, 2009) to identify samples possessing similar PAH compositions within the CAA. We adopted the Aitchison distance as a measure of similarity between the samples and the Ward method (minimum-variance method) for agglomerative calculation purposes. The FCM algorithm requires in-advance specification of the overall number of clusters to be detected. R package NbClust (Charrad *et al.*, 2014) was employed to apply 23 indices and to determine the optimum number of clusters. The FCM clustering results are visualized in silhouette and principal coordinate ordination plots (Kaufman and Rousseeuw, 2009). The silhouette plot allows visualization of the robustness of clusters, where negative values indicate an incorrect and/or questionable assignment (Borcard *et al.*, 2011). Moreover, principal component analysis (PCA) was performed using the PAH data and FCM clustering results with the goal of determining PAH associations with similar relative variation patterns (von Eynatten *et al.*, 2003; Montero-Serrano *et al.*, 2010). FCM clustering analyses was conducted with R software (R Core Team, 2020) using the compositions (van den Boogaart and Tolosana-Delgado, 2008) and cluster packages (Maechler *et al.*, 2019). PCA was conducted with Compositional Data Package (CODAPAK) software (Comas and Thió-Henestrosa, 2011). Finally, the FCM clustering results and PAH concentrations were analyzed to produce distribution maps using Ocean Data View software (Schlitzer, 2015). These maps were generated using a weighted-average gridding algorithm with a quality limit of 1.5. Diagnostic ratios of fluoranthene over the sum of fluoranthene and pyrene (Fla/[Fla+Pyr]) and benz(a)anthracene over the sum of benz(a)anthracene and chrysene (BaA/[BaA+Chr]) were considered to draw boxplots and discriminate PAH sources (i.e., pyrogenic vs petrogenic).

4. RESULTS AND DISCUSSION

4.1 FCM clustering analysis

The FCM clustering analysis results indicate that there are three regional PAH clusters within the CAA (Figs. 6A and S3). Cluster 1 (PAH C#1, red) is mostly representative of the western CAA. Yunker *et al.* (1996) showed that the Mackenzie River imposed a dominant influence on the sedimentary dynamics in this region, namely, all their samples collected from the Mackenzie River, the Mackenzie Shelf and the Beaufort Sea Shelf edge clustered together, agree with our results. This cluster also seems to be dominated more by both medium molecular weight PAHs (MMW = 4-5 rings) and light molecular weight PAHs (LMW = 2-3 rings). This cluster exhibits a higher influence of high molecular weight PAHs (HMW= 6 rings) than the other clusters, however HMW PAHs are minor contributors to the clusters (Fig. 6B). Clusters 2 (PAH C#2, green) and 3 (PAH C#3, blue) are slightly less defined. However, cluster 2 tends to be more represented by LMW PAHs and samples from the eastern CAA, while cluster 3 is more represented by LMW to MMW PAHs (and samples retrieved from the central CAA, as shown in Fig. 6B).

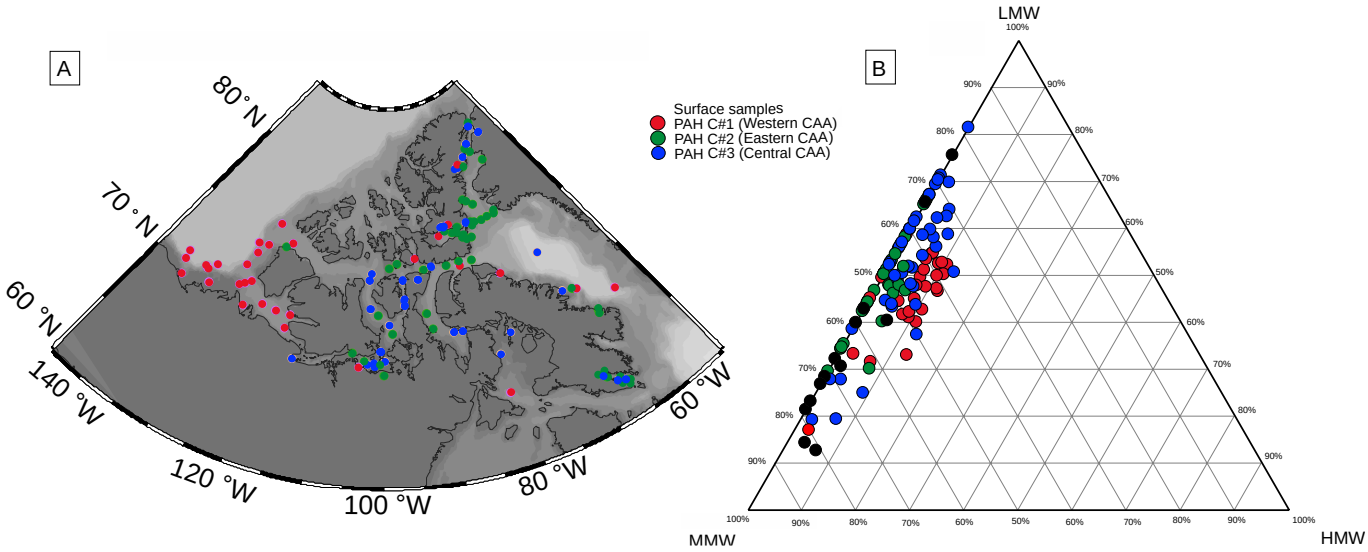

Fig. 6. (A) Fuzzy clustering results for the surface samples. (B) Ternary diagram for the surface and terrestrial samples (black dots) regarding low molecular weight (LMW, 2-3 rings), medium molecular weight (MMW, 4-5 rings) and high molecular weight (HMW, 6 rings) parent PAHs

The ordination diagram and silhouette plot show the robustness of the FCM clustering analysis performed above and corroborate that the CAA can be divided into three main PAH clusters (Fig. 7 and S4). Indeed, 91% of the samples were correctly classified, as indicated by their positive membership values (0.11 to 0.17; Fig. 7B). The other 9% of the samples have negative membership values, indicating an incorrect and/or questionable classification (Fig. 7B). These samples show a greater mix between the PAH C#2 and PAH C#3, suggesting a mixture of PAHs assemblages and sources for the central and eastern CAA.

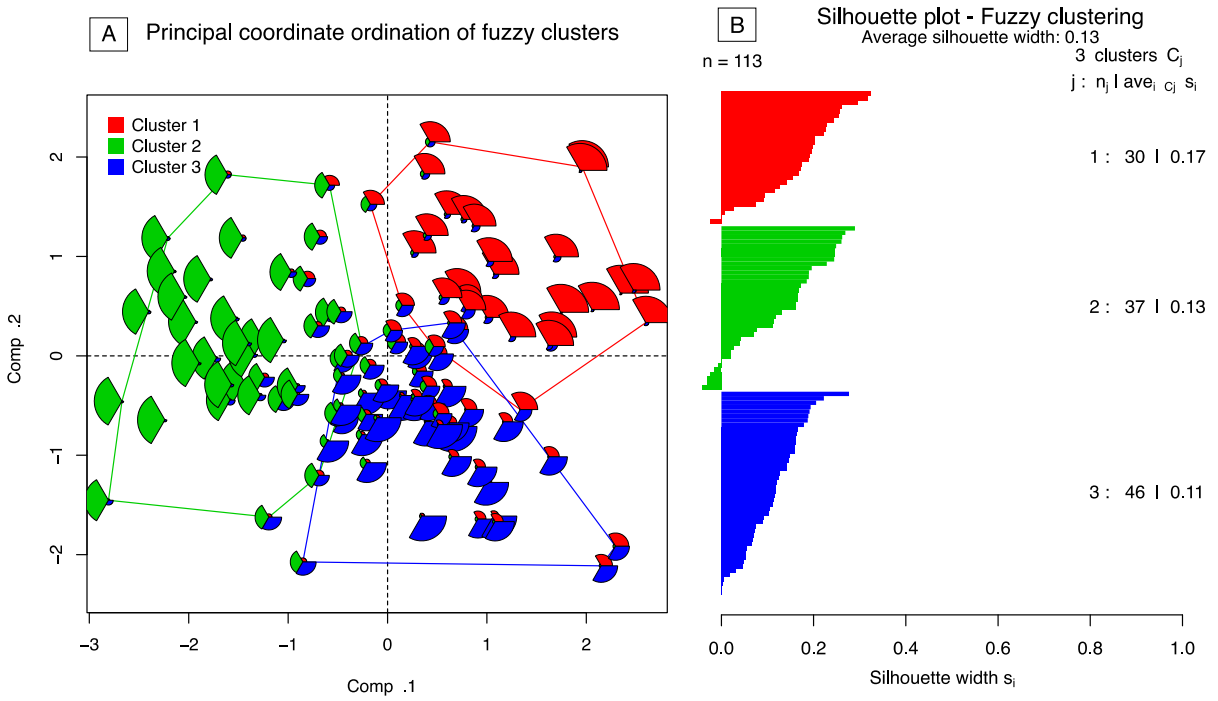

Fig. 7. (A) Ordination of the fuzzy clusters (principal coordinate analysis, PCoA). (B) Silhouette plot for fuzzy clustering of the surface samples based on PAH concentration. The number of samples per clusters and their membership values are listed on the right-hand side of Fig. 7B

4.2 Distribution of TOC and PAHs in recent sediment

The TOC content in the surface sediment samples from the CAA was less than 2 % (Fig. 8A). The PAH C#1 and the PAH C#3 both have an average TOC content of 1 % while the PAH C#2 has a lower average value of 0.7 %. Samples taken in highly biologically productive areas, such as the Mackenzie Shelf, and the Lancaster Sound, the Cape Bathurst and the North Water polynyas (Smith *et al.*, 1997; Tremblay et al., 2006; Barber and Massom, 2007; Simpson *et al.*, 2013a,b), exhibit a higher TOC content (Fig. 8A). Furthermore, the sums of the concentrations of the 16 priority PAHs (Σ_{16}PAHs, dry weight, or dw) designated by the US EPA in the surface sediments of the CAA ranged from 7.8 to 247.7 ng g^{-1} with a mean value of 56.8 ng g^{-1} (Fig. 8; Table 2). The highest values of Σ_{16}PAHs are found in the western CAA, with values ranging from 15.7 to 247.7 ng g^{-1} and a mean value of 107.9 ng g^{-1} (Fig. 9A). The non-parametric Spearman rank method was used to measure the

correlation between the TOC and the PAHs contents in each cluster (Fig. 9B). A significant positive correlation between the TOC and the PAH contents for the three clusters was obtained (R=0.41 to 0.64, p<0.005), suggesting that the TOC plays an important role in the PAHs distribution of the study area and that the Arctic sediments are a suitable sink for PAHs.

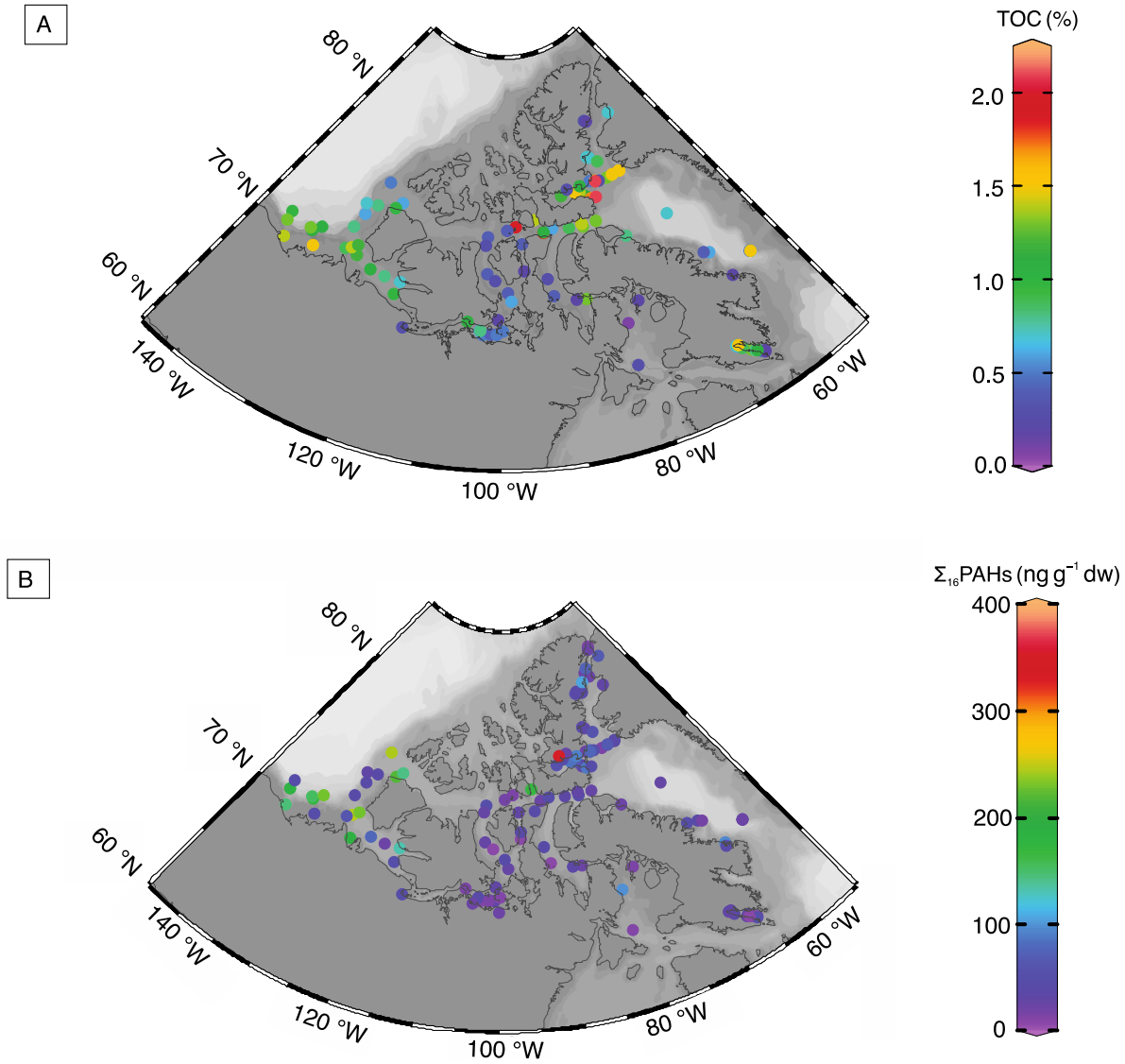

Fig. 8. (A) Spatial distribution of the TOC (%) content in surface sediments from the CAA. (B) Spatial distribution of Σ_{16}PAHs (ng g^{-1} dw) in surface and terrestrial sediments from the CAA

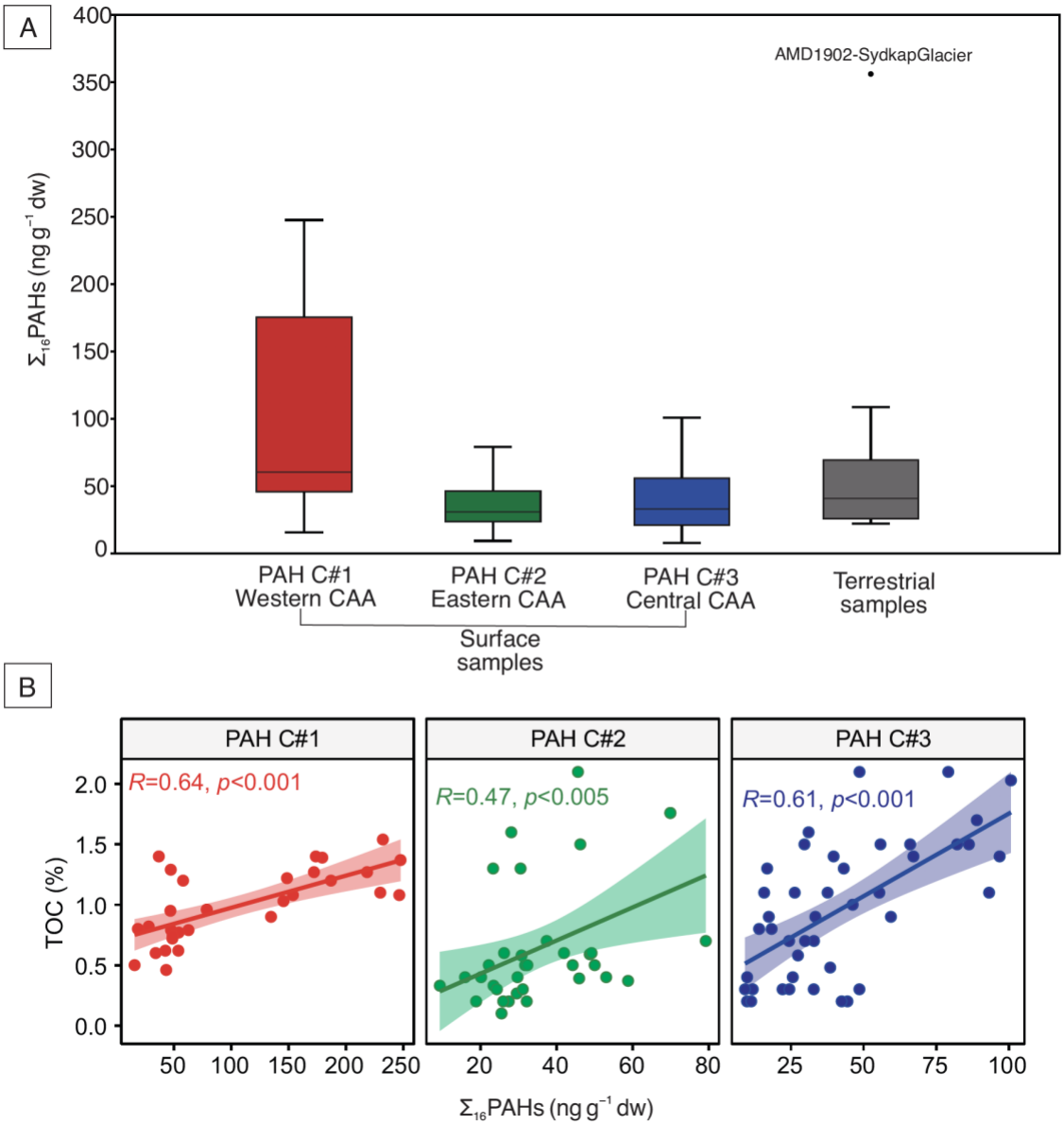

Fig. 9. (A) Box plots of Σ_{16}PAHs (ng g^{-1} dw) in sediments from the CAA separated by cluster. (B) Relation between the TOC (%) and Σ_{16}PAHs in each PAH cluster

According to the values reported in the literature (Table 2), it seems that the seafloors near the Mackenzie River are naturally rich in PAHs, which has been previously explained by the river discharge of the Mackenzie River (Yunker *et al.*, 2002a). Indeed, the river alone discharges an annual flux of 49 ± 8 tons of both particulate and dissolved PAHs onto the

Mackenzie Shelf (Yunker *et al.*, 1991). Additionally, the western CAA is well known for three areas of natural hydrocarbon seeps (oil and/or gas) along the Mackenzie River, Delta and Shelf (Thomas, 1979; Janicki, 2001; Yunker *et al.*, 2002a). The Beaufort Shelf and Mackenzie Shelf are also known for their pockmarks and mud volcanoes releasing fluids and gas into the water column (Blasco *et al.,* 2006; Walsh *et al.,* 2006). Certain on-land seeps, such as the Smoking Hills (Cape Bathurst, Northwest Territories), also release smoke clouds and fumaroles containing PAHs that are then transported by wind (Klungsøyr *et al.*, 2010). The western CAA also has a past history of petroleum exploration. Indeed, from the 1960s to the 1990s, extensive drilling was performed in the Mackenzie/Beaufort Basin, and many sumps for drilling wastes were built, which have leaked since their abandonment. Hence, accidental oil spills have occurred, but the total inputs are much lower than those from other sources (Klungsøyr *et al.,* 2010). This natural hydrocarbon-rich background and petroleum exploration/extraction activity could explain the relatively high concentrations observed in the Mackenzie River area. Overall, the surface sediment concentrations of Σ_{16}PAHs reported in other studies for the Canada Basin (58.9 – 75.9 ng g^{-1}; Ma *et al.,* 2017) and the Chukchi Sea/Canada Basin (102 ng g^{-1}; Yunker *et al.,* 2011 and 8.8 – 78.3 ng g^{-1}; Ma *et al.,* 2017) are comparable to those reported here for the western CAA but lower than those reported for the Mackenzie Shelf /Mackenzie Shelf edge (495 – 755 ng g^{-1}; Yunker and MacDonald, 1995).

In the two other regions of the CAA, the value of Σ_{16}PAHs (dw) remains low: 7.8 to 100.7 ng g^{-1} with a mean value of 40.8 ng g^{-1} for the eastern CAA and 9.3 to 79.2 ng g^{-1} with a mean value of 35.5 ng g^{-1} for the central CAA (Fig. 9A). These results are similar to other Arctic regions, such as the Kara Sea, the Barents Sea or the Svalbard coast, but higher than the reported values for the Makarov Basin or the Central Arctic Ocean (Table 2). Dong *et al.* (2015) pointed out a decreasing tendency of the PAH concentration with increasing latitude, which could explain why higher PAH concentrations occur in the CAA than those at other northerly sites (e.g., the Canada and Makarov Basins). Another known hydrocarbon seep is located in the eastern CAA along Baffin Island at Scott Inlet (Levy, 1978), but the sample collected near this area does not exhibit a higher concentration than those exhibited

by the other samples collected from the eastern CAA. The values of Σ_{16}PAHs (dw) for the terrestrial samples (i.e., glacial till and river samples) are consistent with those for the marine sediments, with values ranging from 22.1 to 108.8 ng g^{-1} and a mean value of 71.1 ng g^{-1} (Fig. 9A), which are fairly low values. However, a major exception of 356.1 ng g^{-1} is found for the sample collected near the Sydkap Glacier, located approximately 60 km west of the Grise Fiord, the northernmost Inuit community in the CAA (Fig. 8B). It is the highest result among all the samples. No anthropogenic activities or historical accidental spills have been recorded in this area. However, Ellesmere Island is known for its numerous coal deposits (Ricketts and Embry, 1984; Kalkreuth, 2004; Harrison *et al.*, 2011). Coal layers outcrop along the Stenkul Fiord, literally meaning the Coal Fiord, which is part of the Eureka Sound Group coals and occurs approximately 60 km north of the Grise Fiord (Kalkreuth *et al.*, 1996). Thus, such outcropping along the watershed and river shores surrounding the Sydkap area could explain the high PAH concentrations observed in this area.

Table 2. Comparison of the Σ_{16}PAHs of the US EPA in marine sediments of the CAA and other Arctic regions

Region	**$\sum_{16}$PAHs (ng g^{-1} dw)**	**Reference**
Chukchi Plateau	41.6	Dong *et al.*, 2015
Makarov Basin	2.0	
Canada Basin	58.9 – 75.9 (68.3)	Ma *et al.*, 2017
Chucki Sea	8.8 – 78.3 (49.7)	
Central Arctic Ocean	5.8 – 33.9 (13.07)	
North Baffin Bay	25.6 – 199.4 (105.9)	Foster *et al.*, 2015
Beaufort Sea/Canada Basin	412	Yunker *et al.*, 2011
Chukchi Sea/Canada Basin	102	
Mackenzie Shelf	755	

Table 2. (suite)

Mackenzie Shelf Edge	495	Yunker *et al.*, 2011
Canada Basin	27.66 – 167.48	Chen *et al.*, 2018
Canada Basin Makarov Basin	71.4 – 150.2 (115.7) 36.9 – 74.2 (59.5)	Zhao *et al.*, 2016
Kara Sea	ND - 110	Sericano *et al.*, 2001
Svalbard coastal sediments	25 - 38	Jiao *et al.*, 2009
Barents Sea	31.6 – 245.2 (114.3)	Boitsov *et al.*, 2009b
Western CAA Central CAA Eastern CAA Total CAA Terrestrial sediments	15.7 – 247.7 (107.9) 7.8 – 100.7 (40.8) 9.3– 79.2 (35.5) 7.8 – 247.7 (56.8) 22.1 – 108.8 (71.1)	This study

Note: mean values, if available, are in parentheses.

4.3 Historical tendencies of PAHs inputs to sediments

Fig. 10 shows the vertical distribution (0 – 10 cm) of the sums of the concentrations of the 16 priority US EPA PAHs (Σ_{16}PAHs, dw) in 8 sediment cores retrieved from the CAA. The values of Σ_{16}PAHs in all sediment cores range from 8.1 to 191.1 ng g^{-1}.

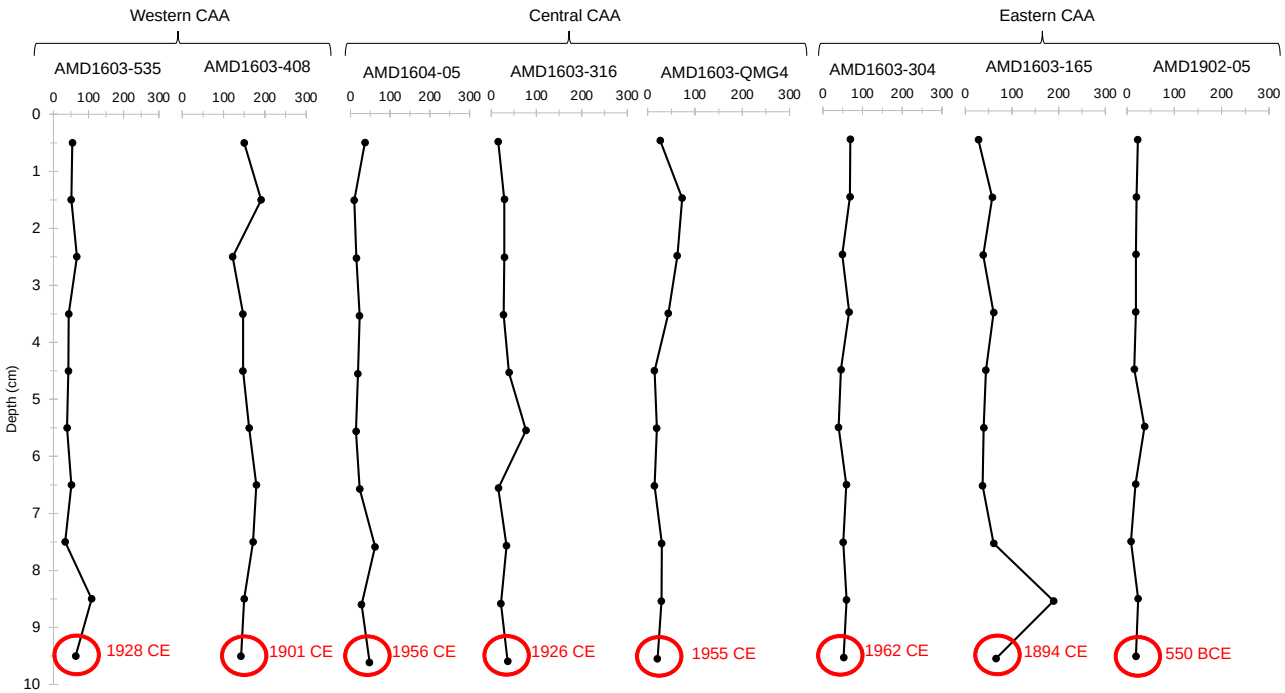

Fig. 10. Profiles of Σ_{16}PAHs (ng g^{-1}, dw) in the selected box cores from western to eastern CAA and the estimated age (CE and BCE) at a core depth of 10th cm is indicated in red

In general, the inputs of PAHs during the last century seem to have remained relatively constant. The value of Σ_{16}PAHs (dw) stays within the general concentrations observed in the surface sediments of the CAA, and none of them is higher than the maximum value of 246.6 ng g^{-1} encountered in the marine sediments in this study. In regard to the surface sediments, the highest sums are found in the western CAA, especially for AMD1603-408, with a mean value of 156.2 ng g^{-1}. Very low values are obtained for AMD1902-05 (a mean value of 20.0 ng g^{-1}), a core collected near Alert (Nunavut, Canada) at the very extreme north of Ellesmere Island. This is consistent with the general trend of the decreasing PAH concentration in the sediments with increasing latitude, since remote locations are far from industrial activities, and the PAH inputs stemming from remote sources are only influenced by long-range atmospheric transport (Dong *et al.*, 2015; Balmer *et al.*, 2019). Additionally, it should be noted that in marine sediments, trends commonly tend to be less defined mainly

because of ocean perturbations (e.g., currents or ship traffic; AMAP, 2017). Therefore, variations due to worldwide fluctuations might indicate a time shift, especially because processes involving ocean currents could last years, whereas atmospheric processes are more common on a daily scale (Klungsøyr *et al.*, 2010). The PAH inputs occurring during the last century are therefore relatively stable. In sediments collected from the Barents Sea, Boitsov *et al.* (2009b) measured a 10-fold increase in the PAH concentration in marine sediments corresponding to the 1910-1940 period, while the inputs prior to 1850 remained constant. After approximately 1980, the concentration slightly decreased. This general decreasing tendency has been associated with a reduction in the worldwide PAH emissions since 1995 (Shen *et al.*, 2013). However, we do not observe this situation in our results. Additionally, Foster *et al.* (2015) studied pre-1900 and post-1900 sediments retrieved from the Baffin Bay area. The majority of their results is within a factor of 10 from those obtained for the post-1900 sediments, indicating a constant PAH concentration over time, which is consistent with our results.

4.4 Source of PAHs for recent and historic sediment

4.4.1 Diagnostic ratios

The ratio of fluoranthene over the sum of fluoranthene and pyrene (Fla/[Fla+Pyr]) and the ratio of benz(a)anthracene over the sum of benz(a)anthracene and chrysene (BaA/[BaA+Chr]) have been successfully applied in previous Arctic studies to determine the PAH sources in recent and preindustrial sediments (e.g., Yunker *et al.*, 2002b; Foster *et al.*, 2015). Typically, Fla/(Fla+Pyr) ratios below 0.4 are representative of petrogenic PAHs, those between 0.4 and 0.5 are representative of fossil fuel combustion and those above 0.5 are representative of biomass combustion (Yunker *et al.*, 2002b). In regard to the BaA/(BaA+Chr) ratio, a value below 0.2 indicates a petrogenic source, a value ranging from 0.2 and 0.35 indicates a mixed source (i.e., either fossil fuel or biomass combustion) and a value above 0.35 indicates a pyrogenic source (Yunker *et al.*, 2002b).

In regard to the surface samples retrieved from the western CAA, the Fla/(Fla+Pyr) values ranged from 0.14 to 0.56, and the BaA/(BaA+Chr) values ranged from 0.13 to 0.33, indicating a mainly petrogenic origin (Fig. 11) with a small influence of mixed combustion origins. This is in agreement with the results reported for the Mackenzie River basin (Yunker *et al*., 2002a, 2011), suggesting that erosion of the organic-rich rocks of the Devonian Canol formation in the lower Mackenzie River valley contributes large amounts of petrogenic hydrocarbons to the shelf. Additionally, the hydrocarbon sources of the Mackenzie Shelf and Canada Basin sediments exhibit a strong signal originating from vascular plants and petrogenic input that is likely to overwhelm a possible combustion signal, leading to a petrogenic signal (Yunker *et al.*, 2011). In the western Arctic Ocean, Ma *et al.* (2017) also reported a mixed petrogenic and pyrogenic source for the PAHs in the surface sediments of the Chukchi Sea and Canada Basin, in line with our results. In the global Arctic Ocean, it has been reported that the natural background signature of petrogenic PAHs seemed to dominate the signal in sediments (Yunker *et al.*, 2011).

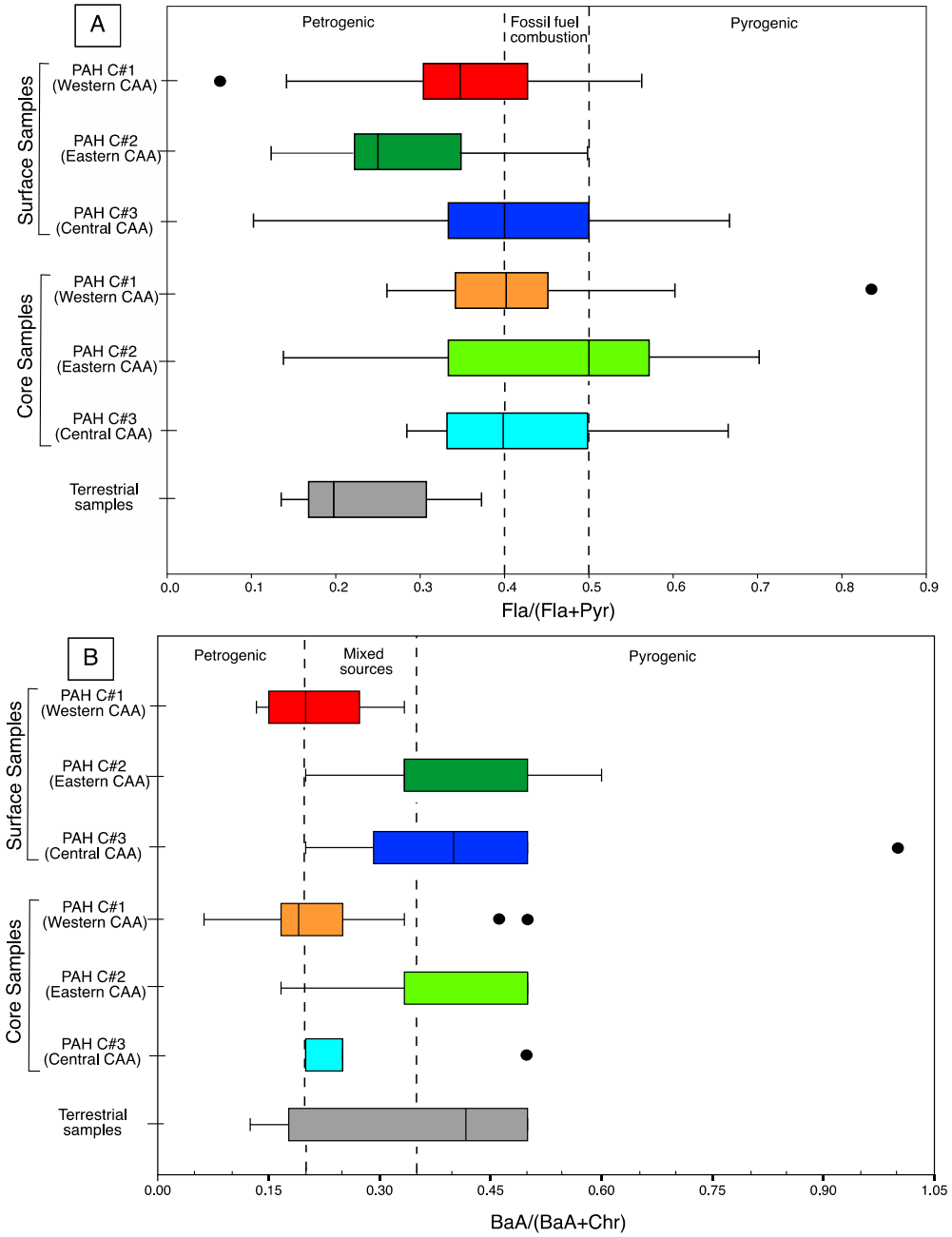

Fig. 11. Diagnostic ratios of the PAH sources: (A) ratio of fluoranthene over the sum of fluoranthene and pyrene (Fla/[Fla+Pyr]). (B) Ratio of benz(a)pyrene over the sum of benz(a)pyrene and chrysene (BaA/[BaA+Chr]) for all samples. The dashed lines indicate the ratio boundaries

Similarly, the surface samples collected from the central CAA appeared to largely exhibit petrogenic signatures, as the Fla/(Fla+Pyr) values ranged from 0.13 to 0.50 (Fig. 11A). However, the BaA/(BaA+Chr) values ranged from 0.20 to 0.60, suggesting a mixed source/pyrogenic source. Regarding the surface samples retrieved from the eastern CAA, the Fla/(Fla+Pyr) values ranged from 0.13 to 0.67, and the BaA/(BaA+Chr) values ranged from 0.20 to 0.50, indicating a well-mixed origin from both petrogenic and pyrogenic sources (Fig. 11). Thus, the central and eastern CAA exhibit a greater pyrogenic influence than the western CAA. It was previously established that the diagnostic ratios for sediments from remote areas might reflect a more pyrogenic influence because the main PAH sources are atmospheric deposition followed by sedimentation (Tsapakis *et al*., 2003; Tobiszewski and Namieśnik, 2012), which could explain our results. Ma *et al.* (2017) and Zhao *et al.* (2016) also reported that the PAHs in samples retrieved from the Arctic Ocean and the Makarov Basin originated from a mixture petroleum and biomass combustion. However, although diagnostic ratios are useful for discriminating the origin of PAHs, they should be interpreted with caution due to different environmental processing of the isomers during transport processes (e.g., Galarneau, 2008; Yunker *et al.*, 2002a,b, 2011). For example, degradation and/or transformation occurring during atmospheric processes and transport through the water column of the less stable fluoranthene and benz(a)anthracene might contribute to bias in old sediments (Yunker *et al.*, 2002a, 2002b, 2011). Tobiszewski and Namieśnik (2012) also suggested that the ratio of Fla/(Fla+Pyr) was more conservative than other ratios (e.g., BaA/[BaA+Ch] and anthracene over the sum of anthracene and phenanthrene; Ant/[Ant+Phe]) during atmospheric photoreactions.

Pyrogenic PAHs stemming from anthropogenic combustion have been widely detected in atmospheric samples retrieved from remote areas in the Arctic, such as Alert (Yu *et al.*, 2019). Modeling studies have shown that long-range atmospheric transport of PAHs from urban areas to remote Arctic regions occurs (Chen *et al.*, 2018). More specifically, air mass trajectory modeling performed at Alert (Nunavut, Canada) has suggested that the atmospheric PAHs in this region mainly originate from Eurasia, North

Europe and North America, while East China is a minor contributor (Wang *et al.*, 2010). Hence, the main anthropogenic PAH source in the Canadian Arctic is the atmospheric deposition of PAHs stemming from worldwide hydrocarbon consumption (Klungsøyr *et al.*, 2010; Yunker *et al.*, 2011). It has also been proposed that local anthropogenic sources are actually negligible compared to deposition from remote sources (e.g., Rose *et al.*, 2004; Wang *et al.*, 2010).

In addition, forest fires are also a contributor to atmospheric pyrogenic PAHs, with an annual budget of approximately 9 tons in the Canadian Arctic, and pyrogenic PAHs have become more frequently detected in atmospheric samples since 2005 (Klungsøyr *et al.*, 2010; Yu *et al.*, 2019). Ma *et al.* (2017) found a pyrogenic influence in deep ocean sediments of the central Arctic Ocean stemming from forest fire events. These events could explain the pyrogenic signal observed in the central and eastern CAA, especially since forest fire events had increased in Canada. For example, the average annual burned area was approximately 1 million hectares in the early 1920s and reached 2 million hectares in the 2010s, with a maximum area of 2.75 million hectares in the 1990s (Wildland Fire Management Working Group, 2013). In Frobisher Bay, near Iqaluit, it appears that anthropogenic activities could locally contribute to pyrogenic PAHs in the bay (Fig. S6). The city, home to more than 7700 people, produces its electricity via imported diesel fuel (Government of Canada, 2017). In 2017, its main greenhouse gas emission sectors were the transportation, industry and electricity sectors (Government of Canada, 2017), all contributing to a pyrogenic signature. Waste burning in Iqaluit is also a common practice (Giroux, 2014), and episodic landfill fire events might contribute to a local PAH input: in 2010, a landfill fire lasted 6 weeks (Harvey, 2018), while another major fire occurred between May and September in 2014 (Weichenthal *et al.*, 2015). Finally, the petrogenic signature recorded near Sydkap Glacier confirms a coal origin (Fla/[Fla+Pyr] = 0.16) rather than an anthropogenic source, as previously reported (Fig. S6).

Regarding the core samples, they all seem to exhibit a mainly petrogenic signature combined with mixed sources: the Fla/(Fla+Pyr) values range from 0.13 to 0.88, and the BaA/(BaA+Chr) values range from 0.16 to 0.50 (Figs. 11 and S5). These values are consistent with the results obtained for the surface samples, except for the eastern CAA core samples, in which the pyrogenic side is more abundant. Overall, it seems that the PAH sources over time have remained relatively constant since the core sample results are consistent with the surface sample results but feature a greater pyrogenic influence. Finally, the terrestrial samples exhibit Fla/(Fla+Pyr) values ranging from 0.14 to 0.38, which indicate a petrogenic source, whereas the BaA/(BaA+Chr) values range from 0.12 to 0.50, indicating a relatively wide range of sources, from petrogenic to mixed/pyrogenic sources. Since only 30% (n=4) of the terrestrial samples attained a BaA/(BaA+Chr) value compared to 85% (n=11) of the samples in regard to Fla/(Fla+Pyr), this pyrogenic influence might not be representative of all the terrestrial samples. However, if it is representative of the 4 samples, it might indicate a more direct connection between atmospheric pyrogenic PAHs and soils since the sedimentary processes do not occur and that soils are mainly influenced by atmospheric deposition (Mostert *et al.*, 2010).

Finally, the results given by the diagnostic ratios should be considered with care given the unknown effect of environmental processes occurring between the emissions and deposition/sedimentation of the PAHS (Tobiszewski and Namieśnik, 2012). Katsoyiannis and Breivik (2014) illustrated that basic conditions such as distance from the sources and ambient temperature, have a significant influence on the molecular ratios. Additionally, diagnostic ratios established for a certain type of sediment in urban area might not be directly applicable to remote sediments; indeed, old basin sediments in the Artic Ocean are depleted in reactive and LMW PAHs from combustion related sources, and only fluoranthene, pyrene and PAHS with molecular weights greater than 252 could provide usable source ratios (Yunker *et al.*, 2011). Hence, the contradictory results obtained in this study do not mean that they are wrong: a combination of degradation during atmospheric processes and the remote

locations might explain why the Fla/(Fla+Pyr) and BaA/(BaA+Chr) values are not exactly the same (Tobiszewski and Namieśnik, 2012).

4.4.2 Principal component analysis (PCA)

PCA based on the Σ_{16}PAH data for all samples (surface, core and terrestrial samples) revealed that PC-1 (24% of the total variance) was positively correlated with 9,10-dimethylanthracene, 3,6-dimethylphenanthrene and pyrene, whereas PC-2 (15% of the total variance) was positively correlated with chrysene, 1-methylphenanthrene and pyrene (Fig. 12; Table S4). Finally, PC-3 (14% of the total variance) was positively correlated with 1-methylnaphthalene, 2-methylnaphthalene and acenaphthene (Fig. 12; Table S4). Parent PAHs are typically more closely associated with combustion processes, while alkylated PAHs are generally derived from petrogenic PAHs (Yunker and Macdonald, 1995; Lima *et al.*, 2005, Balmer *et al*., 2019). Hence, each score indicated a mostly petrogenic influence. Additionally, the PC-1 and PC-3 scores were negatively correlated with at least one parent PAH composed of four rings (e.g., pyrene or chrysene). Unsubstituted PAHs containing four to six rings are mainly associated with combustion sources (Laflamme and Hites, 1978). Hence, PCA confirms a mainly petrogenic influence with a small pyrogenic contribution to the PAHs occurring in the surface, core and terrestrial sediments within the CAA.

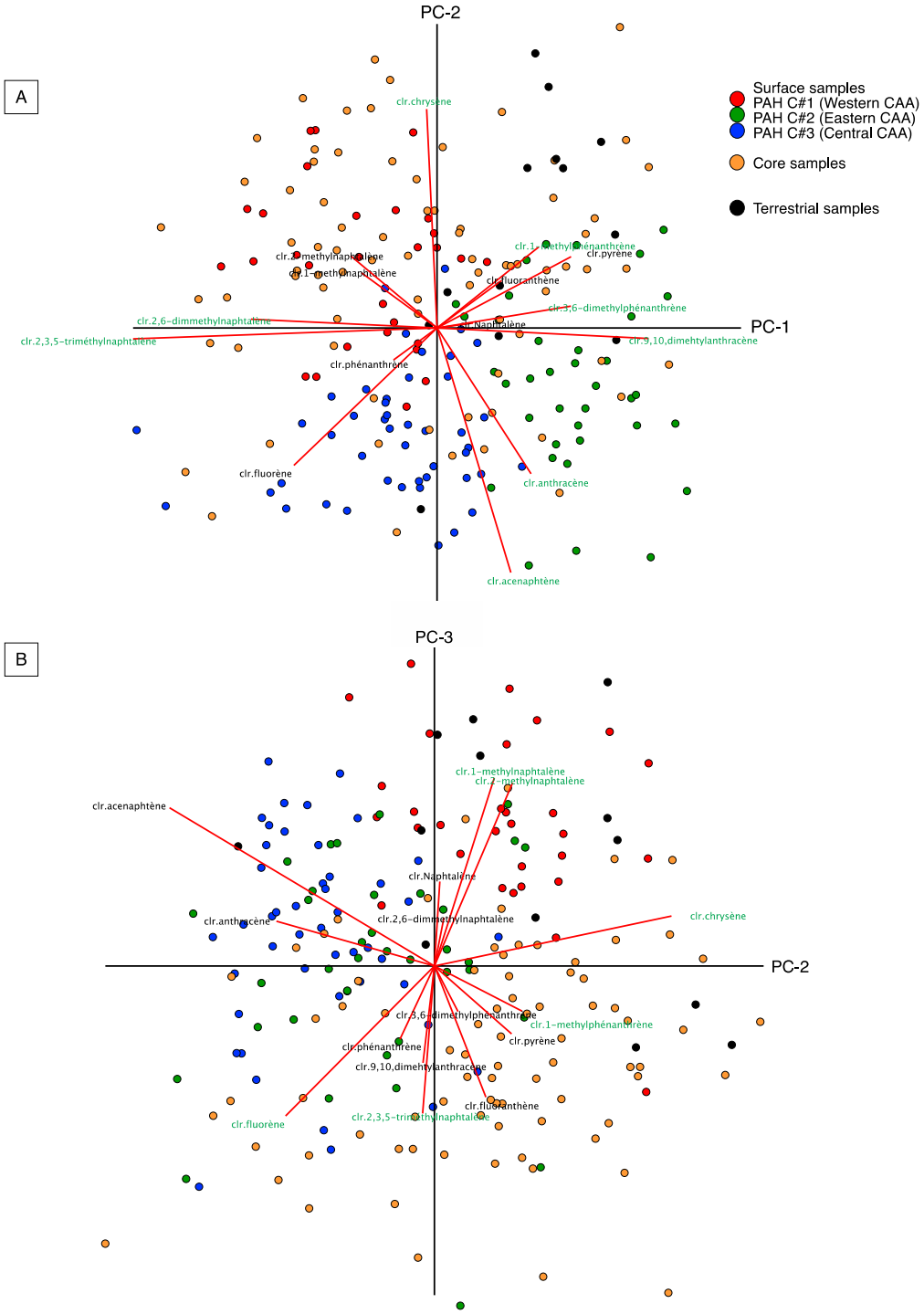

Fig. 12. (A) Biplot of PC-1 versus PC-2. (B) PC-2 versus PC-3 obtained from the log-centred transformation of the PAHs data of the CAA sediments. The PAHs that dominate in each PC score are marked in green

Overall, both diagnostic ratios support the predominant petrogenic nature of the PAHs in the surface sediments of the CAA (Thomas and MacDonald, 2005; Yunker *et al.*, 2011; Foster *et al.*, 2015; Yu *et al.*, 2019). These petrogenic sources are presumably derived from hydrocarbon seeps, weathering of organic-rich rocks, and coastal terrestrially derived material. Strong pyrogenic influences are observed in the central and eastern CAA and are likely due to forest fire events plus long-range atmospheric transport and deposition of PAHs originating from distant sources. Other pyrogenic influence might occur because the remote locations mainly are mainly influenced by deposition of atmospheric pyrogenic PAHs, as previously mentioned. Our results are comparable to those of previous studies pointing to petrogenic sources of the PAHs in the surface sediments of the Mackenzie River/Delta, Beaufort Sea, Nansen Basin, and North Baffin Bay (Yunker *et al.*, 2011, Foster *et al.*, 2015) and mixed sources in the surface sediments of North Baffin Bay, Greenland Sea and north Barents Sea (Yunker *et al.*, 2011; Foster *et al.*, 2015).

4.5 Risk assessment for PAHs

The potential ecological risk of the PAHs in sediments can be determined based on guideline values, such as the effects range-low (ERL, the probability of adverse biological effects is <10%) and effects range-median (ERM, the probability of adverse biological effects is >50%) values, as proposed by Long *et al.* (1995). The PAH content ranges in the CAA sediments are almost all below the ERL and ERM values (Table 3), indicating that the measured PAHs pose a low ecological risk to the benthic organisms or other organisms living near the sediments. Only fluorene might be an exception and would require greater attention. The sample with a result of 23.7 ng g^{-1} is located in the Amundsen Gulf. This result excludes the next highest value for fluorene is 15.9 ng g^{-1}, and all samples are therefore below the above ERL and ERM values.

Table 3. Risk assessment of the PAHs in the sediments retrieved from the study area

Compound	Content range (ng g^{-1} dw)			ERL	ERM
	Surficial sediments	Terrestrial sediments	Core sediments		
Naphthalene	ND - 27.2	3.9 - 20.5	0.0 - 13.7	160	2100
2-Methtlnaphthalene	ND - 36.1	2.0 - 13.4	0.0 - 22.1	70	670
Acenaphthylene	ND - 3.0	0.0 - 2.2	0.0 - 0.3	44	640
Acenaphthene	0.0 - 9.1	0.0 - 2.2	0.0 - 5.9	16	500
Fluorene	0.0 - 23.7	0.0 - 11.2	ND - 12.1	19	540
Phenanthrene	0.0. - 63.5	0.0 - 10.1	ND - 61.2	240	1500
Anthracene	ND - 8.9	ND - 9.0	ND - 4.5	85.3	1100
Fluoranthene	0.0 - 23.7	0.0 - 40.3	0.0 - 28.4	600	5100
Pyrene	0.0 - 79.5	2.8 - 205.9	ND - 81.3	665	2600
Benz(a)anthracene	ND - 7.8	ND - 6.0	ND - 16.3	261	1600
Chrysene	2.9 - 42.2	0.0 - 30.0	ND - 22.1	384	2800
Benzo(a)pyrene	0.0 - 96.7	0.0 - 11.0	0.0 - 29.8	430	1600
Dibenz(a,h)anthracene	0.0 - 6.3	0.0 - 11.0	0.0- 3.7	63.4	260

ND = Not detected; ERL and ERM values from Long *et al.*, 1995.

5. CONCLUSIONS

This study provides a robust baseline record of the PAHs in surface and core marine sediments and terrestrial sediments retrieved from the CAA. The results of this research yield the following generalizations and conclusions:

1. The CAA is divided into three areas with distinct PAH compositions: (a) the western CAA, characterized by MMW (4-5 rings) with a small influence of HMW (6 rings) PAHs; (b) the central CAA, characterized by MMW to LMW (2-3 rings) PAHs; and (c) the eastern CAA, characterized by MMW PAHs.

2. The total organic carbon content in the sediments samples is less than 2% for all the CAA: the western and eastern CAA exhibit a mean value of 1% while the central CAA exhibits a mean value of 0.7%. The sums of the concentrations of the 16 priority PAHs designated by

the US EPA in both the marine and terrestrial sediments of the CAA are fairly low and comparable to other sediment levels reported for Arctic remote regions. Indeed, our results reveal Σ_{16}PAH values ranging from 7.8 to 247.7 ng g^{-1} for the total CAA, while the terrestrial sediments exhibit values ranging from 23.1 to 108.8 ng g^{-1}. Overall, regarding Σ_{16}PAHs, the different regions are classified as follows: central CAA < eastern CAA < terrestrial sediments < western CAA. The PAH contents are also positively correlated to the TOC contents for the three clusters. Additionally, the values of Σ_{16}PAHs in the sediments are all below the ERL and ERM guidelines, except for a single sample retrieved from the Amundsen Gulf, which exhibits a fluorene content above the ERL value.

3. The inputs throughout the last century have remained relatively stable and below the maximum sum obtained for the surface sediment samples, with the Σ_{16}PAH values in the core samples ranging from 8.1 to 191.1 ng g^{-1} with a very low Σ_{16}PAH value in the northernmost core located in the Robertson Channel.

4. The diagnostic ratios of Fla/(Fla+Pyr) and BaA/(BaA+Chr), in addition to the PCA results of the PAH data, suggest that the PAHs mainly have a natural petrogenic origin, but the central and eastern CAA areas also contain PAHs originating from both fossil fuel and biomass burning, likely because of the increase in forest fire events in northern Canada in recent decades and long-range atmospheric deposition of PAHs stemming from urban areas located further south. However, diagnostic ratios should be used with care when applied to sediments from remote locations: PAHs might undergo major environmental processes before their deposition, which could lead to bias and complications in interpreting diagnostic ratio values.

6. ACKNOWLEDGMENTS

We sincerely thank the captain, crew and scientific participants of the 2016, 2017, 2018, and 2019 ArcticNet expeditions onboard CCGS Amundsen for the recovery of the

sediment samples used in this study. We would like to thank Quentin Beauvais (ISMER-UQAR) and Steeven Ouellet (UQAR) for all their technical support and advice in the laboratory. We also thank Zhe Lu (ISMER-UQAR) and Yves Gélinas (Concordia University) for their insightful comments on an earlier version of the manuscript as well as the American Journal Experts for the support with the English editing. This study was supported by ArcticNet, Québec-Océan, CREATE ArcTrain program, and the Natural Sciences and Engineering Research Council of Canada (NSERC) through Discovery Grants provided to J.-C. Montero-Serrano and the *Fonds de recherche du Québec - Nature et technologies* (FRQ-NT) MSc scholarship provided to the first author. All analytical data presented will be available electronically in the PANGAEA database (https://www.pangaea.de/).

CRediT authorship contribution statement

Anne Corminboeuf: investigation, writing - original draft.

Jean-Carlos Montero-Serrano: conceptualization, resources, writing – review and editing, funding acquisition.

Richard St-Louis: conceptualization, resources, writing – review and editing.

CONCLUSION GÉNÉRALE

L'étude présentée a permis d'analyser les concentrations en HAPs de 113 échantillons de sédiments marins de surface, de 13 échantillons de sédiments terrestres et de 80 sous-échantillons de sédiments marins issus de 8 carottes à boîte. La répartition des échantillons à travers tout l'AAC a permis de dresser un portrait robuste et global de l'état actuel et passé des concentrations en HAPs dans les sédiments. L'analyse de grappes (cluster) a permis de diviser l'AAC en trois régions ayant une composition en HAPs distincte : (a) l'ouest de l'AAC, dont les HAPs sont principalement de masse moléculaire moyenne (4-5 cycles) à élevée (6 cycles) ; (b) le centre de l'AAC dont les HAPs sont principalement de masse moléculaire moyenne à faible (2-3 cycles) et (c) l'est de l'AAC dont les HAPs sont principalement de masse moléculaire moyenne (Fig. 13).

Les sédiments de l'AAC sont caractérisés par un contenu en carbone organique inférieur à 2%. : l'ouest et l'est de l'AAC présentent une valeur moyenne de 1% tandis que le centre de l'AAC présente une valeur moyenne de 0,7%. Pour tout l'archipel, la somme des concentrations des 16 HAPs prioritaires de l'US EPA varie entre 7,8 et 247,7 ng g^{-1} avec une valeur moyenne de 56,8 ng g^{-1}. La teneur en HAPs est fortement corrélée ($R=0.41$ à 0.64 et $p<0,05$) au contenu en carbone organique pour les trois régions de l'AAC. L'ouest de l'AAC se distingue par des concentrations plus élevées qui varient de 15,7 à 247,7 ng g^{-1} avec une moyenne de 107,9 ng g^{-1}. Cette moyenne plus élevée s'explique principalement par les apports en sédiments riches en HAPs du fleuve Mackenzie vers le plateau du Mackenzie (Yunker *et al.,* 2002a) et par les ressources sous-marines d'hydrocarbures de ce secteur (Walsh *et al.,* 2006; Blasco *et al.,* 2016). Le centre de l'AAC et l'est de l'AAC présentent des concentrations respectives de 7,8 à 100,7 ng g^{-1} (valeur moyenne de 40,8 ng g^{-1}) et de 9,3 à 79,2 ng g^{-1} (valeur moyenne de 35,3 ng g^{-1}). Ainsi, ces deux régions de l'AAC présentent des sommes de concentrations relativement faibles et comparables à d'autres sédiments de régions de l'Arctique subissant peu d'influence anthropique, comme la mer de

Kara, la mer de Barents ou encore les côtes du Svalbard (Sericano *et al.,* 2001; Boitsov *et al.,* 2009a; Jiao *et al.,* 2009). Les Σ_{16}HAPs pour les sédiments terrestres se maintiennent dans les valeurs obtenues pour les sédiments marins, avec des valeurs entre 22,1 et 108,8 ng g^{-1} (valeur moyenne de 71,7 ng g^{-1}). Concernant les apports en HAPs au cours des années 1920 à 2020, l'analyse des 10 premiers centimètres de 8 carottes sédimentaires a donné des Σ_{16}HAPs variant de 8,1 à 191,1 ng g^{-1} et dont les teneurs sont restées relativement constantes puisqu'aucune valeur n'excède celles rapportées pour les sédiments de surface. De plus, les Σ_{16}PAHs dans les sédiments sont toutes sous les valeurs de références pouvant mener à des effets biologiques néfastes (ERL et ERM), à l'exception d'un seul échantillon provenant du Golfe d'Amundsen qui présente une concentration en fluorène supérieure à la valeur ERL suggérée.

En ce qui a trait aux sources de HAPs, l'utilisation de 2 ratios diagnostiques (fluoranthène sur la somme de fluoranthène et de pyrène ainsi que benz(a)anthracène sur la somme de benz(a)anthracène et de pyrène) a permis de mettre en évidence des sources principalement pétrogénique, donc naturelles. Les résultats pointant du côté des sources pyrogéniques pour le centre de l'AAC et l'est de l'AAC peuvent s'expliquer par le transport atmosphérique sur longue distance permettant aux HAPs anthropiques, et donc surtout pyrogéniques, émis en Amérique du Nord de s'y retrouver, mais aussi aux évènements de feux de forêt qui sont de plus en plus fréquents et intenses dans le nord du Canada depuis les dernières décennies (Klungsøyr *et al.,* 2010; Yunker *et al.*, 2011; Wildland Fire Management Working Group, 2013; Yu *et al.,* 2019). Lorsque les sources sont regardées d'un point de vue temporel, elles restent encore une fois relativement constantes et pointent vers des apports majoritairement pétrogéniques en plus d'une influence pyrogénique (Fig. 13).

Finalement, les trois facteurs de l'analyse de composantes principales (PC-1, PC-2 et PC-3) sont positivement corrélés à des HAPs alkylés représentatifs des réserves sous-marines de gaz et de pétrole, et donc cohérents avec des sources pétrogéniques. Deux des facteurs (PC1 et PC-3) sont négativement corrélés à des HAPs composés de 4 cycles. Ces derniers étant associés à des sources de combustion permettent de confirmer une influence surtout

pétrogénique pour tout l'AAC, mais avec une certaine influence pyrogénique à cause des facteurs PC-1 et PC-2 positivement corrélés au pyrène, un HAP constitué de 4 cycles indicateur d'une influence pyrogénique.

Notre étude a donc permis de dresser un portrait complet de la distribution spatiale et temporelle des HAPs prioritaires de l'US EPA dans une grande partie de l'AAC. La série de données fournies par ce projet pourrait être complétée par des analyses ultérieures permettant de dresser un portrait géochimique des sédiments de l'AAC encore plus complet. Entre autres, des analyses concernant les concentrations en métaux lourds (e.g., mercure, cadmium et plomb) ou de polluants organiques persistants (e.g., composés organochlorés, composés perfluorés) pourraient s'ajouter afin d'évaluer les niveaux de distribution pré ouverture du Passage du Nord-Ouest, surtout que ce sont des composés ciblés par le Programme de lutte contre les contaminants dans le nord (PLCN) du gouvernement du Canada (Gouvernement du Canada, 2018). Des analyses détaillées de la matière organique pourraient s'ajouter afin de déterminer les bassins sédimentaires les plus à risque d'accumuler les HAPs. Finalement, des analyses sur les concentrations en HAPs dans l'atmosphère, la glace de mer et la matière particulaire en suspension dans l'AAC pourraient s'ajouter afin d'évaluer le couplage qui s'effectue aux interfaces air-eau et eau-sédiments et la cohérence entre la teneur en HAPs des particules en surface vs la teneur des sédiments profonds.

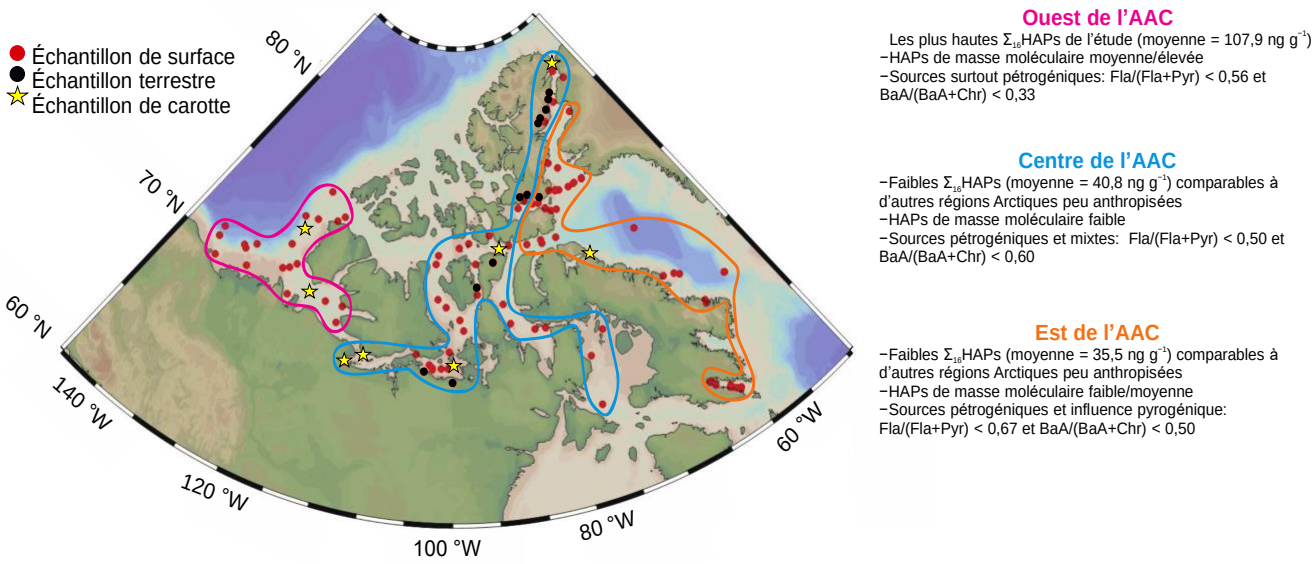

Fig. 13. Résumé des caractéristiques reliées aux HAPs des trois clusters définis dans cette étude

ANNEXES

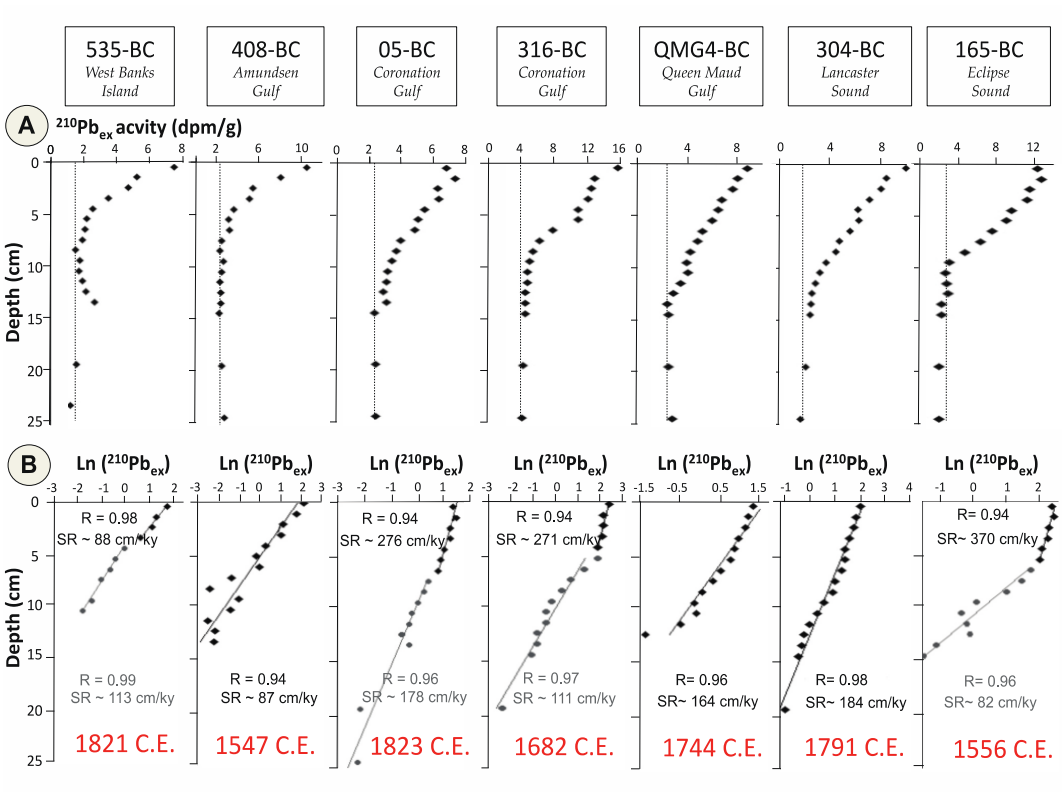

Fig. S1. ^{210}Pb chronology of the 8 box cores from the CAA studied here. The sedimentation rates (SR) used to calculate the basal age for each sediment core is also shown (Letaïef, 2019)

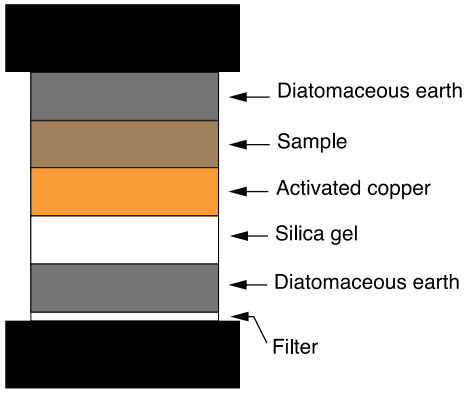

Fig. S2. Packing of the extract cell (adapted from Choi *et al.*, 2014)

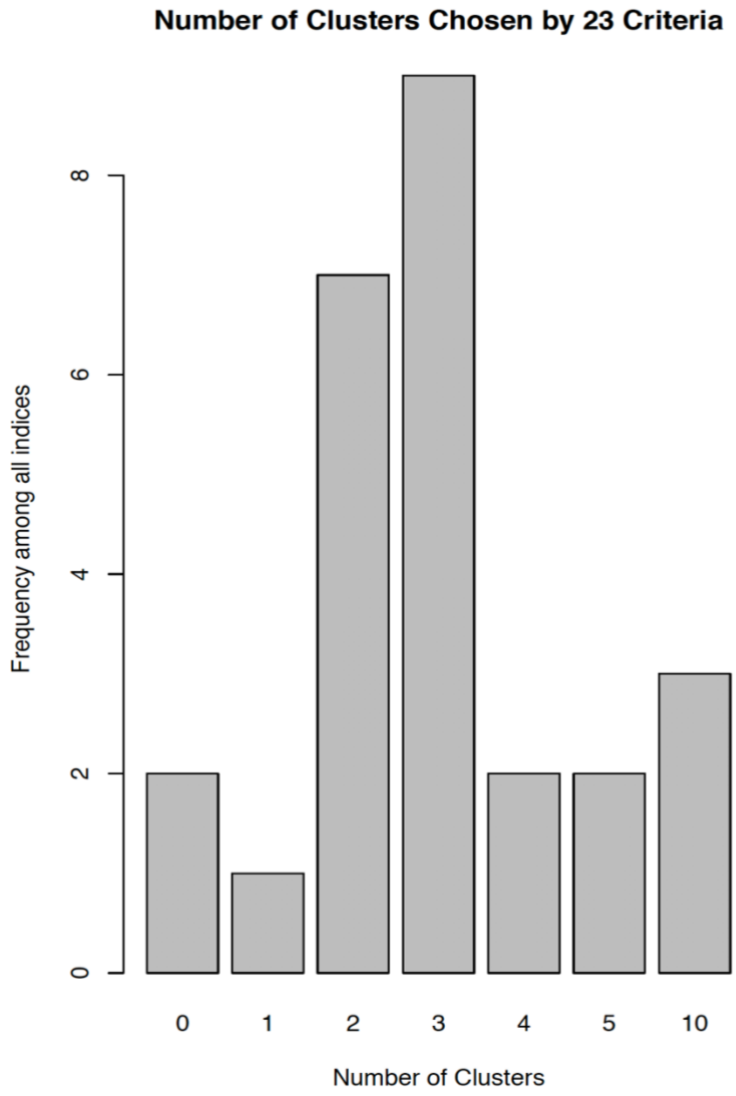

Fig. S3. NbClust result showing that the optimal number of clusters is 3

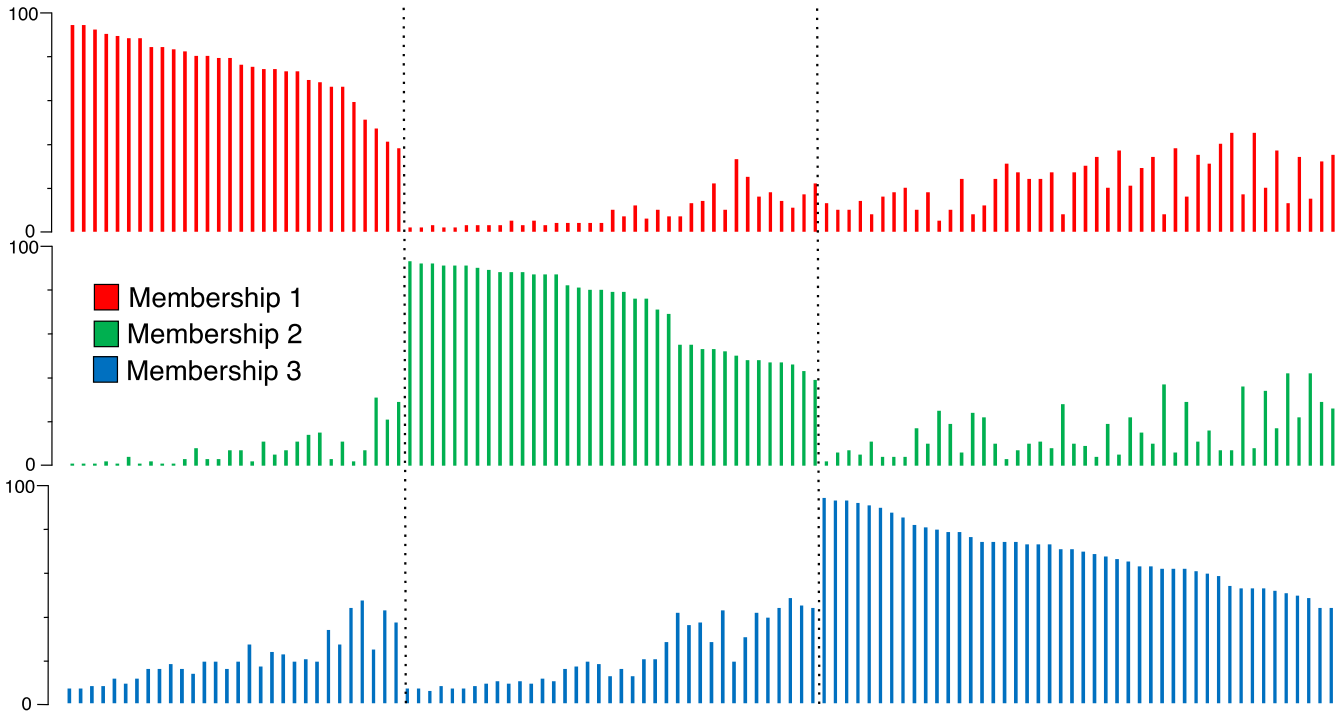

Fig. S4. Percent of samples associated with the three clusters determined in this study. The plot indicates that most of the surface samples were correctly classified, whereas 1 sample from cluster 1, 6 samples from cluster 2 and 2 samples from cluster 3 might be incorrectly classified. This is likely due to their PAHs assemblages and sources.

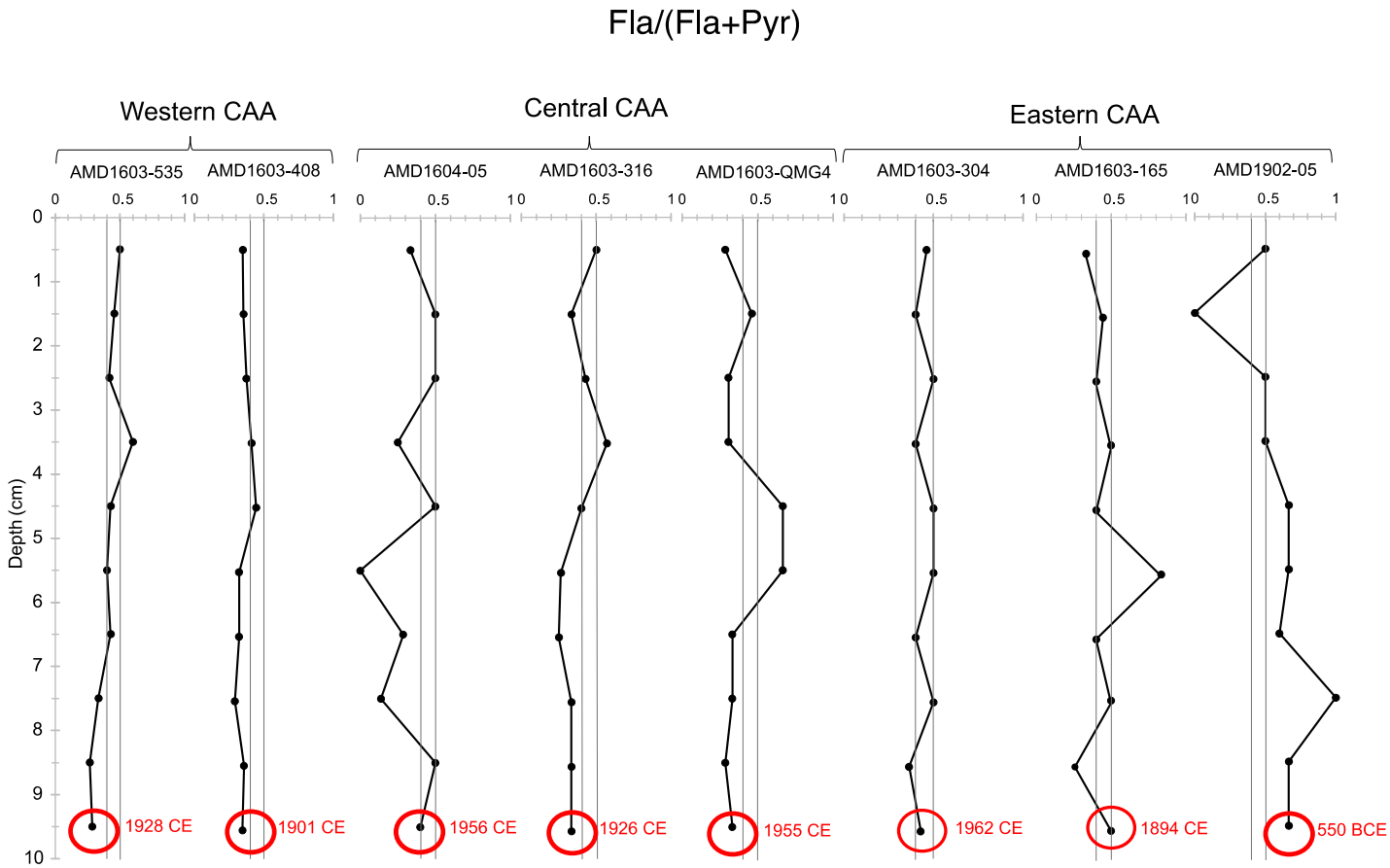

Fig. S5. Ratio of fluoranthene over the sum of fluoranthene and pyrene (Fla/[Fla+Pyr]) in the core sediments. The solid lines indicate ratio boundaries of 0.4 and 0.5. Red indicates the calculated age (CE or BCE) at 10 cm of the core

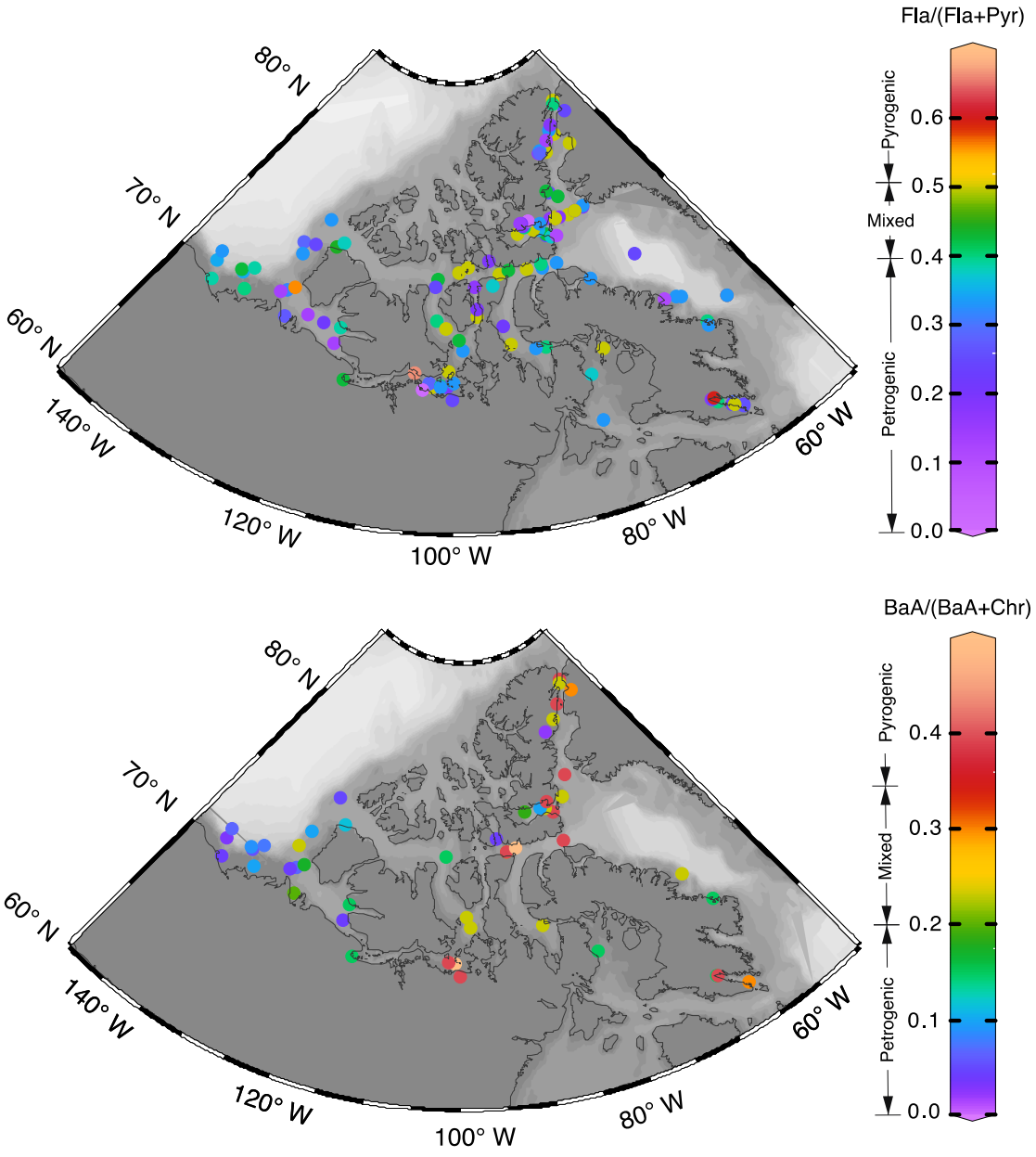

Fig. S6. Spatial distribution of Fla/(Fla+Pyr) and BaA/(BaA+Chr) in the CAA sediments

Table S1. Comparison between the spike-corrected recoveries for certified reference material NIST-1944 between this sudy and the reference study of Choi *et al.* (2014)

Compound	**Mean recovery value (%) for this study (n=20)**	**Mean recovery value (%) for the reference study**
Naphthalene	31.8	46.1
1-Methylnaphthalene	66.6	65.4
2-Methylnaphthalene	30.2	50.5
Acenaphthene	37.2	56.1
Fluorene	38.0	34.1
Phenanthrene	86.6	82.4
Anthracene	75.7	56.6
Fluoranthene	88.6	95.3
Pyrene	78.4	80.9
Benz(a)anthracene	67.8	69.9
Chrysene	83.8	84.7
Benzo(b)fluoranthene	82.7	82.7
Benzo(k)fluoranthene	70.1	73.6
Benzo(a)pyrene	66.2	10.0
Indeno(1,2,3-c,d)pyrene	29.8	91.3
Dibenz(a,h)anthracene	121.7	145.0
Benzo(g,h,i)perylene	62.1	101.0

Table S2. Method detection limit (MDL) calculated based on the 7 replicates

Compound	Concentration obtained by the GC-MS µg mL^{-1}							Standard deviation	MDL µg mL^{-1} (x 3.143)	MDL * ng g^{-1}
	1	2	3	4	5	6	7			
Naphtalene	0.47	0.41	0.47	0.49	0.52	0.50	0.52	0.0353	0.111	12.7
1-Methylnaphthalene	0.43	0.35	0.46	0.46	0.51	0.49	0.50	0.0506	0.159	18.2
1-Methylnaphthalene-d10	0.11	0.09	0.13	0.12	0.12	0.14	0.13	0.0151	0.048	5.4
2-Methylnaphthalene	0.47	0.36	0.50	0.49	0.50	0.46	0.51	0.0478	0.150	17.2
2,6-Dimethylnaphthalene	0.09	0.09	0.11	0.12	0.12	0.13	0.12	0.0146	0.046	5.2
Acenaphthylene	0.85	0.74	0.89	0.88	1.02	0.97	0.97	0.0868	0.273	31.2
Acenaphthene	0.44	0.35	0.44	0.45	0.50	0.48	0.46	0.0440	0.138	15.8
2,3,5-Trimethylnaphthalene	0.11	0.10	0.12	0.10	0.12	0.11	0.12	0.0083	0.026	3.0
Fluorene	0.09	0.07	0.09	0.09	0.10	0.09	0.09	0.0083	0.026	3.0
Phenanthrene	0.05	0.03	0.05	0.04	0.04	0.05	0.05	0.0073	0.023	2.6
Anthracene	0.04	0.03	0.05	0.05	0.05	0.04	0.05	0.0073	0.023	2.6
1-Methylphenanthrene	0.11	0.09	0.12	0.12	0.12	0.11	0.13	0.0118	0.037	4.2
3,6-Dimethylphenanthrene	0.12	0.08	0.11	0.12	0.11	0.11	0.11	0.0125	0.039	4.5
Fluoranthene	0.16	0.12	0.15	0.18	0.18	0.17	0.17	0.0196	0.062	7.0
Pyrene	0.02	0.02	0.02	0.02	0.05	0.04	0.03	0.0112	0.035	4.0
9,10-Dimethylanthracene	0.10	0.08	0.10	0.08	0.12	0.11	0.12	0.0155	0.049	5.6
Benz(a)anthracene-d12	0.07	0.05	0.07	0.08	0.09	0.06	0.07	0.0120	0.038	4.3
Benz(a)anthracene	0.03	0.02	0.03	0.03	0.03	0.02	0.03	0.0045	0.014	1.6
Chrysene	0.03	0.02	0.03	0.03	0.05	0.03	0.04	0.0088	0.028	3.2
Benzo(b)fluoranthene	0.03	0.03	0.04	0.03	0.04	0.05	0.06	0.0107	0.034	3.8
Benzo(k)fluoranthene	0.03	0.01	0.02	0.02	0.01	0.03	0.02	0.0076	0.024	2.7
Benzo(a)pyrene	0.01	0.01	0.02	0.02	0.01	0.02	0.02	0.0049	0.016	1.8
Indeno(1,2,3-c,d)pyrene	0.02	0.02	0.03	0.03	0.03	0.02	0.03	0.0049	0.016	1.8
Dibenz(a,h)anthracene	0.03	0.03	0.05	0.05	0.04	0.03	0.04	0.0083	0.026	3.0
Benzo(g,h,i)perylene	0.07	0.03	0.06	0.05	0.05	0.04	0.03	0.0139	0.044	5.0

* A calculation example is presented after this table

Calculation example to convert the concentration obtained with the GC-MS (µg mL^{-1}) to a concentration of PAHs in sediments (ng g^{-1})

$$[PAHs\ sediments] = \frac{\frac{[GC-MS] * V_{tot.vial}}{V_{samp}} * V_{evap}}{w_{sed}} * 1000$$

Where:

[PAHs sediments]: concentration of PAHs in sediments (ng g^{-1})

[GC-MS]: concentration obtained with the GC-MS (µg mL^{-1})

$V_{tot.vial}$: total volume of the vial used for the GC-MS injection (mL)

V_{samp}: volume of the sample used for the GC-MS injection (mL)

V_{evap}: final volume of the sample after the evaporation (mL)

w_{sed}: weight of sediments used for the ASE extraction (g)

1000: conversion factor from µg to ng

Example for the determination of the MDL for the Naphthalene, where [GC-MS] = 0.111 µg mL^{-1}

$$MDL = \frac{\frac{0.111\ ug\ mL^{-1} * 0.2\ mL}{0.175\ mL} * 0.5\ mL}{5\ g} * \frac{1000\ ng}{\mu g}$$

$$MDL = 12.7\ ng\ g^{-1}$$

Table S3. Content range (ng g^{-1}, dw) for each PAH

Compound	Surficial sediments			Terrestrial Sediments	Core Sediments
	Western Archipelago	Central Archipelago	Eastern Archipelago		
Naphthalene	3.0 - 27.2 (14.5)	ND - 8.0 (4.2)	1.5 - 3.8 (4.1)	3.9 - 20.5 (8.8)	0.0 - 13.7 (4.6)
1-Methylnaphthalene	4.4 - 52.0 (24.5)	ND - 13.9 (3.8)	0.0 - 8.0 (3.3)	2.0 - 17.9 (6.7)	0.0 - 22.7 (4.3)
2-Methtlnaphthalene	3.0 - 36.1 (19.3)	ND - 9.9 (2.5)	0.0 - 8.6 (2.6)	2.0 - 13.4 (5.9)	0.0 - 22.1 (3.9)
2,6-Dimethylnaphthalene	2.3 - 26.0 (12.0)	0.0 - 5.6 (1.8)	0.0 - 14.7 (2.5)	0.0 - 6.7 (2.2)	0.0 - 15.9 (3.5)
Acenaphthylene	0.0 - 3.0 (1.1)	ND	ND - 1.5 (0.1)	0.0 - 2.2 (0.2)	0.0 - 0.3 (0.3)
Acenaphthene	1.2 - 9.1 (4.2)	0.0 - 7.4 (2.0)	0.0 - 7.5 (1.8)	0.0 - 2.2 (0.6)	0.0 - 5.9 (1.0)
2,3,5-Trimethylnaphthalene	1.0 - 23.1 (8.0)	0.0 - 6.0 (1.2)	ND - 25.1 (2.5)	0.0. - 4.5 (1.0)	0.0 - 22.7 (4.2)
Fluorène	0.0 - 23.7 (6.2)	0.0 - 7.0 (1.5)	0.0 - 13.9 (2.8)	0.0 - 11.2 (2.5)	ND - 12.1 (3.0)
Phenanthrene	8.9 - 63.5 (33.3)	2.3 - 23.8 (8.7)	0.0 - 33.3 (9.5)	0.0 - 10.1 (3.7)	ND - 61.2 (13.0)
Anthracene	1.2 - 7.8 (2.8)	ND - 8.9 (1.6)	0.0 - 8.3 (1.4)	ND - 9.0 (1.8)	ND - 4.5 (1.0)
1-Methylphenanthrene	2.3 - 30.5 (9.4)	0.0 - 11.9 (2.7)	ND - 11.6 (2.1)	0.0 - 20.1 (4.1)	ND - 14.4 (3.4)
3,6-Dimethylphenanthrene	1.5 - 21.7 (7.6)	0.0 - 9.9 (3.1)	0.0 - 14.9 (2.8)	0.0 - 58.2 (7.7)	0.0 - 17.0 (3.0)
Fluoranthene	0.0 - 23.7 (1.2)	1.2 - 9.0 (3.2)	0.0. - 19.9 (4.1)	0.0 - 40.3 (6.0)	0.0 - 28.4 (5.6)
Pyrene	4.1 - 30.7 (15.8)	0.0 - 18.5 (8.0)	1.4 - 79.5 (8.0)	2.8 - 205.9 (27.2)	ND - 81.3 (9.6)
9,10-Dimethylanthracene	0.0 - 13.8 (5.2)	0.0 - 13.4 (3.6)	0.0 - 14.4 (2.7)	1.9 - 17.6 (6.4)	0.0 - 14.3 (3.3)
Benz(a)anthracene	ND - 7.8 (4.2)	ND - 2.5 (0.5)	ND - 3.9 (0.9)	ND - 6.0 (1.1)	ND - 16.3 (1.5)
Chrysene	2.9 - 42.2 (18.1)	0.0 - 11.4 (2.4)	0.0 - 19.1 (2.7)	0.0 - 30.0 (5.9)	ND - 22.1 (5.3)
Benzo(b)fluoranthene	ND - 18.2 (4.3)	ND - 7.1 (0.7)	ND - 40.6 (2.2)	ND - 18.3 (6.8)	ND - 10.1 (1.6)
Benzo(k)fluoranthene	ND - 17.4 (3.7)	ND - 5.7 (0.7)	0.0 - 4.8 (0.9)	ND - 2.6 (0.6)	ND - 13.6 (2.4)
Benzo(a)pyrene	0.0 - 96.7 (8.5)	0.0 - 34.2 (1.6)	0.0 - 48.5 (4.0)	0.0 - 11.0 (2.3)	0.0 - 29.8 (5.3)
Indeno(1,2,3-c,d)pyrene	0.0 6.3 (2.4)	ND - 1.5 (0.1)	ND - 1.7 (0.2)	ND - 1.5 (0.2)	ND - 3.7 (0.4)
Dibenz(a,h)anthracene	0.0 - 6.3 (2.4)	0.0 - 1.5 (0.1)	ND - 1.2 (0.0)	0.0 - 11.0 (1.7)	ND - 3.7 (0.3)
Benzo(g,h,i)perylene	0.0 - 22.5 (9.7)	0.0 - 7.6 (0.9)	ND - 4.0 (1.2)	ND - 10.5 (1.5)	ND - 22.2 (2.1)

Note: in parentheses are the mean values.

ND = not detected

Table S4. Variance in the samples explained and loadings of the three significant factors determined via PCA

Compounds	PC1 24%	PC2 15%	PC3 14%
Naphthalene	0.07	0.01	0.19
1-Methylnaphthalene	-0.14	0.13	0.43
2-Methylnaphthalene	-0.17	0.17	0.42
2,6-Dimethylnaphthalene	-0.36	0.02	0.11
Acenaphthene	0.14	-0.59	0.36
2,3,5-Trimethylnaphthalene	-0.58	-0.03	-0.34
Fluorene	-0.27	-0.33	-0.34
Phenanthrene	-0.08	-0.08	-0.17
Anthracene	0.18	-0.35	0.10
1-Methylphenanthrene	0.19	0.20	-0.10
3,6-Dimethylphenanthrene	0.26	0.05	-0.10
Fluoranthene	0.12	0.11	-0.30
Pyrene	0.26	0.17	-0.15
9,10-Dimethylanthracene	0.40	-0.03	-0.22
Chrysene	-0.02	0.53	0.11

Note : green indicates the 3 highest positive loadings; red indicates the 3 highest negative loadings

RÉFÉRENCES BIBLIOGRAPHIQUES

Alkire, M.B., Jacobson, A.B., Lehn, G.O., Macdonald, R.W., Rossi, M.W. 2017. On the geochemical heterogeneity of rivers draining into the straits and channels of the Canadian Arctic Archipelago. Journal of Geophysical Research: Biogeosciences, 122(10), 2527-2547.

Aitchison, J.1986. The statistical analysis of compositional data. Monographs on statistics and applied Probability: Chapman & Hall, London (Reprinted in 2003 with additional material by Blackburn Press), 416 p.

Aitchison, J. 1990. Relative variation diagrams for describing patterns of compositional variability. Mathematical Geology, 22(4), 487–511.

AMAP, 2010. AMAP Assessment 2007: oil and gas activities in the arctic — effects and potential effects. Arctic Monitoring and Assessment Program, Oslo, vols. 1 and 2.

AMAP, 2017. AMAP Assessment 2016: Chemical of emerging Arctic concern. Arctic Monitoring and Assessment Program (AMAP), Oslo, Norway, (16) 353.

Appleby, P. G., Oldfieldz, F. 1983. The assessment of 210Pb data from sites with varying sediment accumulation rates. Hydrobiologia, 103(1), 29-35.

Askenov, Y., Popova, E.E., Yool, A., George Nurser, A.J., Williams, T.D., Bertino, L., Bergh, J. 2017. On the future navigability of Arctic sea routes: High-resolution projections of the Arctic Ocean and sea ice. Marine Policy 75, 300–317.

Balk, L., Meijer, J., DePierre, J.W., Appelgren, L.-E. 1984. The uptake and distribution of [3H]benzo[a] pyrene in the Northern pike (Esox lucius). Examination by whole-body autoradiography and scintillation counting. Toxicology and Applied Pharmacology, 74, 430–49.

Balmer, J.E., Hung, H., Yu, Y., Letcher, R.J., Muir, D.C.G. 2019. Sources and environmental fate of pyrogenic polycyclic aromatic hydrocarbons (PAHs) in the Arctic. Emerging Contaminants, 5, 128-142.

Barber, D.G., Massom, R.A. 2007. The role of sea ice in Arctic and Antarctic polynyas. In : Smith, W.O., Barber, D.G., eds. Polynyas: Windows to the world. Elsevier Oceanographic Series 74. Amsterdam, Elsevier, 1-54.

Blasco, S., Bennett, R., Kostylev, V., Campbell, P., Shearer, J., Conlan, K. 2006. Seabed topography, geological structure and evolution of the sea-ice regime on the Beaufort Shelf at the western entrance to the Northwest Passage: CCGS Nahidik Research. The

Canadian Geomorphology Research Group, 3rd Annual ArcticNet Scientific meeting. December 12-15, 2006. Victoria, British-Colombia.

Bird, K.J., Charpentier, R.R., Gautier, D.L., Houseknecht, D.W., Klett, T.R., Pitman, J.K., Moore, T.E., Schenk, C.J., Tennyson, M.E., Wandrey, C.J. 2008. Circum-Arctic resource appraisal; estimates of undiscovered oil and gas north of the Arctic Circle: U.S. Geological Survey Fact Sheet 2008-3049, 4 p.

Boitsov, S., Jensen, H.K.B., Klungsøyr, J. 2009a. Geographical variations in hydrocarbon levels in sediments from the Western Barents Sea. Norwegian Journal of Geology, 89, 91-100.

Boitsov, S., Jensen, H.K.B., Klungsøyr, J. 2009b. Natural background and anthropogenic inputs of polycyclic aromatic hydrocarbons (PAH) in sediments of the south-western Barents Sea. Marine Environmental Research, 68, 236-245.

Borcard, D., Gillet, F., Legendre, P. 2011. Numerical ecology with R, Springer, New York.

Charrad, M., Ghazzali, N., Boiteau, V., Niknafs, A. 2014. Nbclust: an R package for determining the relevant number of clusters in a data set. Journal of Statistical Software, 61, 1–36.

Chen, F., Lin, Y., Cai, M., Zhang, J., Zhang, Y., Kuang, W., Liu, L., Huang, P., Ke, H. 2018. Occurrence and risk assessment of PAHs in surface sediments from Western Arctic and Subarctic Ocean. International Journal of Environmental Research and Public Health, 15, 734.

Chiou, C.T., McGroddy, S.E., Kile, D.E. 1998. Partition characteristics of polycyclic aromatic hydrocarbons on soils and sediments. Environmental Science & Techonology, 32 (2) 264-269.

Choi, M., Kim., Y.-J., Lee, I.-S., Choi, H.-G. 2014. Development of a one-step integrated pressurized liquid extraction and cleanup method for determining polycyclic aromatic hydrocarbons in marine sediments. Journal of Chromatography A, 1340, 8-14.

Comas, M., Thió-Henestrosa, S. 2011. CoDaPack v2.02.21: a stand-alone, multi-platform compositional software. CoDaWork'11: 4th International Workshop on Compositional Data Analysis 1-10.

Comiso, J.C., Parkinson, C.L., Gersten, R., Stock, L. 2008. Accelerated decline in the Arctic sea ice cover. Geophysical Research Letters 35, L01703. doi:10.1029/2007GL031972.

Darby, D.A. 2003. Sources of sediment found in sea ice from the western Arctic Ocean, new insights into processes of entrainment and drift patterns. Journal of Geophysical Research 108, 1–10.

Darby, D.A., Nyers, W.B., Jakobsson, M. and Rigor, I. (2011). Modern dirty sea ice characteristics and sources: The role of anchor ice. Journal of Geophysical Research, 116,18 pp.

De Laender, F., Hammer, J., Hendricks, A.J., Stoetaert, K., Janssen, C. 2011. Combining monitoring data and modeling identifies PAHs as emerging contaminants in the Arctic. Environmental Science and Technology, 45, 9024-9029.

Dong, C., Bai, X., Sheng, H., Jiao, L., Zhou, H., Shao, Z. 2015. Distribution of PAHs and the PAH-degrading bacteria in the deep-sea sediments of the high-latitude Arctic Ocean. Biogesciences, 12, 2163-2177.

Doucette, J. 2006. Woods Hole Oceanographic Institution, online, URL: https://www.whoi.edu/sbl/liteSite.do?litesiteid=6894&articleId=10666

Dowdeswell, J. A., Hogan, K. A., Arnold, N. S., Mugford, R. I., Wells, M., Hirst, J. P. P., Decalf, C. 2015. Sediment-rich meltwater plumes and ice-proximal fans at the margins of modern and ancient tidewater glaciers: Observations and modelling. Sedimentology, 62(6), 1665–1692.

Foster, K.L., Stern, G.A., Carrie, J., Bailey, J.N.-L., Outridge, P.M., Sanei, H., Macdonald, R.W. 2015. Spatial, temporal, and source variations of hydrocarbons in marine sediments from Baffin Bay, Eastern Canadian Arctic. Science of the Total Environment, 506-507, 430-443.

Galarneau, E. 2008. Sources specificity and atmospheric processing of airborne PAHs: Implication for source apportionment. Atmospheric Environment, 42(35), 8139-8149.

Giroux, L. 2014. State of waste management in Canada. Report prepared for the Canadian Council of Ministers of Environment (CCME). [PDF]: https://www.ccme.ca/files/Resources/waste/wst_mgmt/State_Waste_Mgmt_in_Canada%20April%202015%20revised.pdf

Government of Canada. 2017. Provincial and territorial energy profiles – Nunavut. [URL]: https://www.cer-rec.gc.ca/nrg/ntgrtd/mrkt/nrgsstmprfls/nu-eng.html

Gouvernement du Canada. 2018. Programme de lutte contre les contaminants dans le Nord : contaminants préoccupants, en ligne, [URL] : https://www.ic.gc.ca/eic/site/063.nsf/fra/h_2025D549.html

Gschwend, P.M., Hites, R. 1981. Fluxes of polycyclic aromatic hydrocarbons to marine and lacustrine sediments in the northeastern United States. Geochimica et Cosmochimica Acta, 45, 2359-2367.

Haritash, A.K., Kaushik, C.P. 2009. Biodegradation aspects of polycyclic aromatic hydrocarbons (PAHs): A review. Journal of Hazardous Materials, 169, 1-15.

Harris, P.T. 2012. Seafloor geomorphology – Coast, shelf, and abyss. Seafloor geomorphology as benthic habitat, GeoHAB atlas of seafloor geomorphic features and benthic habitats, 109-155.

Harrison, J.C., St-Onge, M.R., Petrov, O.V., Strelnikov, S.I., Lopatin, B.G., Wilson, F.H., Tella, S., Paul, D., Lynds, T., Shokalsky, S.P., Hults, C.K., Bergman, S., Jepsen, H.F., Solli, A. 2011. Geological map of the Arctic, Geological Survey of Canada, Open Access: https://doi.org/10.4095/287868.

Harvey, M. 2018. Discussions sur le futur dépotoir de la ville d'Iqaluit, dans le nord canadien. Radio-Canada International, [URL]: https://www.rcinet.ca/regard-sur-arctique/2018/11/19/depotoir-iqaluit-dechets-enfouissement-nunavut-enfouissement-pollution/

Hélie, J.-F. (2009). Elemental and stable isotopic approaches for studying the organic and inorganic carbon components in natural samples. IOP Conf. Ser. Earth Environ. Sci. 5, 012005, https://doi.org/10.1088/1755-1307/5/1/012005

Hiscott, R. N., Aksu, A. E., Nielsen, O. B. 1989. Provenance and dispersal patterns, Pliocene-Pleistocene section at site 645, Baffin Bay. Proceedings of the Ocean Drilling Program, Scientific Results, 105, 31-52.

IARC, 1987. IARC Monographs on the Evaluation of the Carcinogenic Risk of Chemicals to Humans. Overall Evaluations of Carcinogenicity: An Updating of the IARC Monographs Vol. 1 to 42, Supplement 7. International Agency for Research on Cancer, WHO, Lyon, France.

Janicki, E. 2001. A brief history of hydrocarbons exploration in the North-west Territories. A publication of the C.S. Lord Northern Geosciences Center, North-west Territories Geosciences Center.

Jennings, A.E., Sheldon, C., Cronin, T.M., Francus, P., Stoner, J., Andrews, J. 2011. The Holocene history of Nares Strait: Transition from glacial bay to Arctic-Atlantic throughflow. Oceanography, 24(3), 26-41.

Jiao, L.P., Zheng, G.J., Minh, T.B., Richardson, B., Chen, L.Q., Zhang, Y.H., Yeung, L.W., Lam, J.C.W., Yang, X.L., Lam, P.K.S., Wong, M.H. 2009. Persistent toxic substances in remote lake and coastal sediments from Svalbard, Norwegian Arctic: levels, sources and fluxes. Environmental Pollution, 157, 1342-1351.

Jörrundsdóttir, H.O., Jensen, S., Hylland, K., Holth, T.F., Gunnlaugsdóttir, H., Svavarsson, J., Ólafsdóttir, El-Taliawy, H., Rigét, F., Strand, J., Nyberg, E., Bignert, A., Hoydal, K.S., Pálmar Halldórsson, H. 2014. Pristine Arctic: Background mapping of PAHs, PAH metabolites and inorganic trace elements in the North-Atlantic Arctic and sub-Arctic coastal environment. Science of the Total Environment, 493 (2014) 719-728.

Kalkreuth, W.D., Riediger, C.L., McIntyre, D.J., Richardson, R.J.H., Fowler, M.G., Marchioni, D. 1996. Petrological, palynological and geochemical characteristics of EurekaSound Group coals (Stenkul Fiord, southern Ellesmere Island, Arctic Canada). International Journal of Coal Geology, 30, 151-182.

Kalkreuth, W.D. 2004. Coal facies studies in Canada, International Journal of Coal Geology, 58, 23-30.

Katsoyiannis, A., Breivik, K. 2014. Model-based evaluation of the use of polycyclic aromatic hydrocarbons molecular diagnostic ratios as source identification tool. Environmental Pollution, 184, 488-494.

Kaufman, L., Rousseeuw, P.J. 2009. Finding groups in data: an introduction to cluster analysis, John Wiley & Sons.

Keith, L.H. 2014. The Source of U.S. EPA's sixteen PAH priority pollutants. Polycyclic Aromatic Compounds, 35, 147-160.

Klungsøyr, S.L., Dahle, S., Thomas, D.J. 2010. Sources, inputs and concentrations of petroleum hydrocarbons, polycyclic aromatic hydrocarbons, and other contaminants related to oil and gas activities in the Arctic. In: AMAP Assessment 2007: Oil and gas activities in the Arctic – Effects and Potentiel Effects. Volume 2, chapter 4. Arctic Monitoring and Assessment Programme (AMAP).

Lai, S.YJ., Gerber, T.P., Amblas, D. 2016. An experimental approach to submarine canyon evolution. Geophysical Research Letters, 43 (6), 2741-2747.

Laflamme, R.E., Hites, R.A. 1978. The global distribution of polycyclic aromatic hydrocarbons in recent sediments. Geochimica et Cosmochimica Acta, 41, 289-303.

Lammel, G., Sehili, A. M., Bond, T. C., Feichter, J., Grassl, H. 2009. Gas/particle partitioning and global distribution of polycyclic aromatic hydrocarbons – A modelling approach. Chemosphere, 76(1), 98–106.

Lasserre, F. 2010. Vers l'ouverture d'un Passage du Nord-Ouest stratégique ? Entre les États-Unis et le Canada. Outre-Terre, 25-26 (2), 437-452.

Letaïef, S. 2019. Les processus sédimentaires durant le Petit âge glaciaire et l'actuel dans l'Archipel arctique canadien. Mémoire. Rimouski, Université du Québec à Rimouski, Institut des sciences de la mer de Rimouski (ISMER), 96 p. http://semaphore.uqar.ca/id/eprint/1500/

Levy, E.M. 1978. Visual and chemical evidence for a natural seep at Scott Inlet, Baffin Island, District of Franklin. Geological Survey of Canada, pp. 21-26. Current Research Paper: 78-1B.

Lima, A.L., Farrington, J.W., Reddy, C.M. 2005. Combustion-derived polycyclic aromatic hydrocarbons in the environment – A review. Environmental Forensics, 6, 109-131.

Long, E.R., MacDonal, D.D., Smith, S.L., Calder, F.D. 1995. Incidence of adverse biological effects within ranges of chemical concentrations in marine and estuarine sediments. Environmental Management, 19(1), 81-97.

Ma, Y., Halsall, C.J., Xie, Z., Koetke, D., Mi, W., Ebinghaus, R., Gao, G. 2017. Polycyclic aromatic hydrocarbons in ocean sediments from the North Pacific to the Arctic Ocean. Environmental Pollution, 227, 498-504.

Madaj, L. 2016. Holocene organic carbon and carbonate records from the Northeast Baffin Bay: preliminary age model and paleoenvironmental significance, Msc. Thesis, Department of Earth Sciences, University of Gothenburg, Gothenburg, Sewden, 48p.

Maechler, M., Rousseeuw, P., Struyf, A., Hubert, M., Studer, M., Roudier, P. 2019. Finding Groups in Data: Cluster Analysis Extended Rousseeuw et al. R package. [Available at https://cran.r-project.org/web/packages/cluster/]

Meador, J.P., Stein, J.E., Reichert, W.L., Varanasi, U. 1995. Bioaccumulation of polycyclic aromatic hydrocarbons by marine organisms. Reviews of Environmental Contamination and Toxicology, 143, p.79-164.

Meek, M.E., Chan, P.K.L., Bartlett, S. 1994. Polycyclic aromatic hydrocarbons evaluation of risks to health from environmental exposure in Canada. Journal of Environmental Science Health, Part C: Environmental Carcinogenesis and Ecotoxicological Reviews, 12(2), 443-452.

Melling, H. 2002. Sea ice of the Northern Canadian Arctic Archipelago. Journal of Geophysical Research, 107 (C11) 3181.

Michel, C., Ingram, R.G., Harris, L.R. 2006. Variability in oceanographic and ecological processes in the Canadian Arctic Archipelago. Progress in oceanography, 71, 379-401.

Mojiri, A., Zhou, J.L., Ohashi, A., Ozaki, N., Kindaichi, T. 2019. Comprehensive review of polycyclic aromatic hydrocarbons in water sources, their effects and treatments. Science of the Total Environment, 696, 133971.

Montero-Serrano, J. C., Palarea-Albaladejo, J., Martin-Fernandez, J.-A., Martinez-Santana, M., Gutierrez-Martin, J. V. 2010. Sedimentary chemofacies characterization by means of multivariate analysis. Sedimentary Geology, 228, 218–228, doi:10.1016/j.sedgeo.2010.04.013.

Montero-Serrano, J. C., Rioux P., Aebischer, S. 2016. Natural climate and oceanographic variability in the western Canadian Arctic Ocean since the last deglaciation. ArcticNet Leg 3a Cruise Report - CCGS Amundsen (25 August to 17 September 2016).

Montero-Serrano, J.-C., Furze, M. Zindorf, M., Pieńkowski, A. 2017. The marine sedimentary record of paleoclimate, paleoceanography, and deglacial history in the eastern Canadian Arctic Archipelago and Northern and Eastern Baffin Bay. ArcticNet Leg 2b Cruise Report - CCGS Amundsen (13 July to 17 August 2017).

Montero-Serrano, J.-C., Brossard, J., Corminboeuf, A. 2018. Collecting sedimentary sequences for paleoclimate, paleoceanographic and environmental studies in the eastern Canadian Arctic Archipelago and Baffin Bay. ArcticNet Leg 3 Cruise Report - CCGS Amundsen (16 August to 9 September 2018).

Montero-Serrano, J.-C., Brossard, J., Corminboeuf, A. 2019. Collecting sedimentary sequences and plankton samples in the continental margins from the eastern Canadian Arctic Archipelago. ArcticNet Leg 2b Cruise Report – CCGS Amundsen (25 July to 15 August 2019).

Morillo, E., Romero, A.S., Madrid, L., Villaverde, J., Maqueda, C. 2008. Characterization and sources of PAHs and potentially toxic metals in urban environments of Sevilla (Southern Spain). Water, Air and Soil Pollution, 187, 41–51.

Mostert, M.M.R., Ayoko, G.A., Kokot, S.. 2010. Application of chemometrics to analysis of soil pollutants. Trends in Analytical Chemistry, 29, 430-435.

Neff, J.M. 1985. Polycyclic aromatic hydrocarbons. In: Rand, G.M., Petrocelli, S.R. (Eds.), Fundamentals or aquatic toxicology; Methods and applications. Hemisphere Publishing Corporation, New York, USA, 416-454.

Neff, J. M., Burns, W. A. 1996. Estimation of polycyclic aromatic hydrocarbon concentrations in the water column based on tissue residues in mussels and salmon: An equilibrium partitioning approach. Environmental Toxicology Chemistry/SETAC, 15, 2240-2253

NISDC, National Ice and Snow Data Center. State of the cryosphere: is the Cryosphere sending signals about climate changes? [online], URL: https://nsidc.org/cryosphere/sotc/sea_ice.html#:~:text=The%20Arctic%20sea%20ice%20September,have%20experienced%20near%2Drecord%20lows.

Oblinger Childress, C.J., Foreman, W.T., Connor, B.F., Maloney, T.J. 1999. New reporting procedures based on long-term method detection levels and some considerations for interpretation of water-quality data provided by the U.S. Geological Survey National Water Quality Laboratory. US Geological Survey, open-file report 99-193.

Ó Cofaigh, C., Taylor, J., Dowdeswell, J.A., Pudsey, C.J. 2003. Palaeo-ice streams, trough mouth fans and high-latitude continental slope sedimentation. Boreas, 32, 37–55.

Page, D.S., Boehm, P.D., Douglas, G.S., Bence, A.E., Burns,W.A., Mankiewicz, P.J. 1999. Pyrogenic polycyclic aromatic hydrocarbons in sediments Record Past human activity: a case study in Prince William Sound, Alaska. Marine Pollution Bulletin, 38, 247-260.

Palarea-Albaladejo J., Martin-Fernandez J.A. 2015. zCompositions — R package for multivariate imputation of left-censored data under a compositional approach. Chemometrics and Intelligence Laboratory Systems 143, 85-96.

Pampanin, D.M., Sydnes, M.O. 2017. Petrogenic polycyclic aromatic hydrocarbons in the aquatic environment: analysis, synthesis, toxicity and environmental impact**.** DOI:10.2174/97816810842751170101

Payne, J.F., Fancey, L., Rahimtula, A.D., Porter, E.L. 1987. Review and perspective on the use of mixed function oxygenase enzymes in biological monitoring. Comparative Biochemistry and Physiology, 86C(2), 233-245.

Pelletier, E., Desbiens, I., Sargian, P., Côté, N., Curtosi, A., St-Louis, R. 2008. Présence des hydrocarbures aromatiques polycycliques (HAP) dans les compartiments biotiques et abiotiques de la rivière et du fjord du Saguenay. Revue des sciences de l'eau, 22(2), 235-251.

Rapinski, M., Cuerrier, A., Harris, C., Elders of Ivujivik, Elders of Kangiqsujuaq, Lemire, M. 2018. Inuit perception of marine organisms: from folk classification to food harvest. Journal of Ethnobiology, 38(3), 333-355.

R Core Team. 2020.. R: A language and environment for statistical computing. R Foundation for Statistical Computing, Vienna, Austria. [Available at https://www.R-project.org/]

Reimnitz, E., Clayton, J.R., Kempema, E.W., Payne, J.R., Weber, W.S. 1993. Interaction of rising frazil with suspended particles: tank experiments with applications to nature. Cold Regions Science and Technology 21, 117–135. doi:http://dx.doi.org/10.1016/0165-232X(93)90002-P

Ricketts, B.D., Embry, A.F. 1984. Summary of the geology and resource potential of coal deposits in the Canadian Arctic Archipelago, Bulletin of Canadian Petroleum Geology, 32(4), 359-371.

Rose, N.L., Rose, C.L., Boyle, J.F., Appleby, P.G. 2004. Lake-sediment evidence for local and remote sources of atmospherically deposited pollutants on Svalbard. Journal of Paleolimnology, 31, 499-513.

Roslund, M.I., Grönroos, M., Rantalainen, A.-L., Jumpponen, A., Romantschuk, M., Parajuli, A., Hyöty, H., Laitinen, O., Sinkkonen, A. 2018. Half-lives of PAHs and temporal microbiota changes in commonly used urban landscaping materials. PeerJ DOI 10.7717/peerj.4508

Scott, M., Hansen K. 2016. Sea ice. NASA Earth Observatory, [online], URL: https://earthobservatory.nasa.gov/features/SeaIce

Schlitzer, R. 2015. Ocean Data View.

Sericano, J.L., Brooks, J.M., Champ, M.A., Kennicutt, M.C., Makeyev, V.V. 2001. Trace contaminant concentrations in the Kara Sea and its adjacent rivers, Russia. Marine Pollution Bulletin, 42, 1017-1030.

Shen, H., Tao, S., Wang, R., Wang, B., Shen, G., Li, W., Su, S., Huang, Y., Wang, W., Liu, W., Li, B., Sun, K. 2011. Global trends in PAH emissions from motor vehicles. Atmospheric Environment, 45(12), 2067-2073.

Shen, H., Huang, Y., Wang, R., Zhu, D., Li, W., Guofeng, S., Wang, B., Zhang, Y., Chen, Y., Lu, Y., Chen, H., Li, T., Sun, K., Li, B., Liu, W., Liu, J., Tao, S. 2013. Global Atmospheric Emissions of Polycyclic Aromatic Hydrocarbons from 1960 to 2008 and

Schøyen, H., Bråthen, S. 2011. The Northern Sea route versus the Suez Canal: cases from bulk shipping. Journal of Transport Geography, 19(4), 977–983.

Simonet, Loïc. 2016. Les hydrocarbures de l'Arctique: El Dorado ou chimère? Géoéconomie, 82(5), 73-98.

Simpson, K.G., Tremblay, J.-É., Price, N.M. 2013a. Nutrient dynamics in the western Canadian Arctic. I. New production in spring inferred from nutrient draw-down in the Cape Bathurst Polynya. Marine Ecology Progress Series, 484, 33-45.

Simpson, K.G., Tremblay, J.-É., Brugel, S., Price, N.M. 2013b. Nutrient dynamics in the western Canadian Arctic. II. Estimates of new and regenerated production over the Mackenzie Shelf and Cape Bathurst Polynya. Marine Ecology Progress Series, 484, 47-62.

Smith, W. Jr., Gosselin, M., Legendre, L., Wallace, D., Daly, K., Kattner, G. 1997. New production in the Northeast Water Polynya: 1993. Journal of Marine Systems, 10 (1-4), 199-209.

Smith, L.C., Stephenson, S.R. 2013. New trans-Arctic shipping routes navigable by midcentury. Proceedings of the National Academy of Sciences of the United States of America, 110 (13) E191-E1195.

Sofowote U.M., Hung H., Rastogi A.K., Westgate J.N., Deluca P.F., Su Y., McCarry B.E. 2011. Assessing the long-range transport of PAH to a sub-arctic site using positive matrix factorization and potential source contribution function. Atmospheric Environment, 45 (4) 967-976.

Stark, A., Abrajano, T.Jr., Hellou, J., Metcalf-Smith., J.L. 2003. Molecular and isotopic characterization of polycyclic aromatic hydrocarbons distribution and sources at the international segment of the St. Lawrence River. Organic Geochemistry, 34, 225-237.

Stein, J.E., Hom, T., Varanasi, U. 1984. Simultaneous exposure of English sole (Parophrys vetulus) to sediment-associated zenobiotics: Part 1—uptake and disposition of ^{14}C polychlorinated biphenyls and 3H-benzo[a]pyrene. Marine Environment Ressources, 13, 97–119.

Stein, R. 1991. Organic carbon accumulation in Baffin Bay and paleoenvironment in high northern latitudes during the past 20 m.y. Geology, 19(4), 356-359.

Stein, R. 2008. Arctic Ocean Sediments: Processes, proxies and paleoenvironment. Elsevier, Developments in Marine Geology, vol.2, 591p.

Thomas, D.J. 1979. Seabed releases of gas around the Tingmiark K-91 wellsite in the southern Beaufort Sea. Dome Petroleum Ltd. Calgary, Alberta.

Thomas, D.J., Macdonald, R.W. 2005. A petroleum hydrocarbon budget for the Arctic. Presentation at the AMAP International Symposium on Oil and Gas Activities in the Arctic, pp. xxxiv. St. Petersburg, 13-15 September 2005.

Tobiszewski, M., Namieśnik, J. 2012. PAH diagnostic ratio for the identification of pollution emission sources. Environmental Pollution, 162, 110-119.

Tomy, G.T., Halldorson, G., Chernomas, L., Bestvater, K., Danegerfield, T., Pleskach, K., Stern, G., Atchison, S., Makewski, A. 2014. Polycyclic aromatic hydrocarbons metabolites in Arctic cod (*Boreogadus saida*) from the Beaufort Sea and associative fish health effects. Environmental Science and Technology, 48, 11629-11636.

Tsapakis, M., Stephanou, E.G., Karakassis, I. 2003. Evaluation of atmospheric transport as a nonpoint source of polycyclic aromatic hydrocarbons in marine sediments of the Eastern Mediterranean. Marine Chemistry, 80, 283-298.

Tremblay, C., Bouchard, M., Gagnon, F., Cartier, J.-F., Bégin, P., Larouche, L. et Dionne, L. 2000. Les hydrocarbures aromatiques polycycliques : exposition et risques dans la population générale, [online] URL : https://www.inspq.qc.ca/es/node/1137

Tremblay J.-É., Michel, C., Hobson, K.A., Gosselin, M., Price N.M. 2006. Bloom dynamics in early opening waters of the Arctic Ocean. Limnology and Oceanography, 51, 900−912a

Tuvikene, A., Huuskonen, S., Roy, S., Lindstrom-Seppa, P. 1996. Biomonitoring of South Estonian waters by means of xenobiotic metabolism of rainbow trout (Oncorhynchus mykiss) liver. Comparative Biochemistry and Physiology, 114C, 71-177.

Van den Boogaart, K. G., Tolosana-Delgado, R. 2008. “Compositions”: a unified R package to analyze compositional data. Computers & Geosciences, 34(4), 320-338.

von Eynatten, H., Barceló-Vidal, C., Pawlowsky-Glahn, V. 2003. Sandstone composition and discrimination: A statistical evaluation of different analytical methods: Journal of Sedimentary Research, 73(1), 47-57.

Van Schooten, F.J. 1991. Polycyclic aromatic hydrocarbon - DNA adducts in mice and humans. Academic thesis, State University of Leiden, The Netherlands.

Xue, W., D. Warshawsky. 2005. Metabolic activation of polycyclic and heterocyclic aromatic hydrocarbons and DNA damage: a review. Toxicology and Applied Pharmacology, 206:73-93.

Yanik, P.J., O'Donnell, T.H., Macko, S.A., Qian, Y., Kennicutt II, M.C. 2003.The isotopic compositions of selected crude oil PAHs during biodegradation. Organic Geochemistry, 34, 291–304.

Yu, Y., Katsoyiannis, A., Bohlin-Nizzetto, P., Brorström-Lundén, E., Ma, J., Zhao, Y., Wu, Z., Tych, W., Mindham, D., Sverko, E., Barresi, E., Dryfhout-Clark, H., Fellin, P., Hung, H. 2019. Polycyclic aromatic hydrocarbons not declining in Arctic air despite global emission reduction. Environmental Science & Technology, 53, 2375-2382.

Yunker, M.B., Macdonald, R.W., Fowler, B.R., Cretney, W.J., Dallimore, S.R., McLaughlin, F.A. 1991. Geochemistry and fluxes of hydrocarbons to the Beaufort Sea Shelf: A multivariate comparison of fluvial inputs and coastal erosion of peat using principal component analysis. Geochimica et Cosmochimica Acta, 55, 255-273.

Yunker, M.B., Macdonald, R.W. 1995. Composition and origins of polycyclic aromatic hydrocarbons in the Mackenzie River and on the Beaufort Sea shelf. Arctic, 48(2), 118-129.

Yunker, M.B., Snowdon, L.R., Macdonald, R.W., Smith, J.N., Fowler, M.G., Skibo, D.N., Mclaughlin, F.A., Danyushevskaya, A.I., Petrova, V.I., Ivanov, G.I. 1996. Polycyclic aromatic hydrocarbons composition and potential sources for sediment samples from the Beaufort and Barents Sea. Environmental Science & Technology, 30(4), 1310-1320.

Yunker, M.B., Backus, S.M., Graf Pannatier, E., Jeffries, D.S., Macdonald, R.W. 2002a. Sources and significance of alkane and PAH hydrocarbons in Canadian arctic rivers. Estuarine, Coastal and Shelf Science, 55, 1–31.

Yunker, M.B., Macdonald, R.W., Vingarzan, R., Mitchell, R.H., Goyette, D., Sylvestre, S. 2002b. PAHs in the Fraser River basin: a critical appraisal of PAH ratios as indicators of PAH source and composition. Organic Geochemistry, 33, 489-515.

Yunker, M.B., Macdonald, R.W., Snowdon, L.R., Fowler, B.R. 2011. Alkane and PAH biomarkers as tracers of terrigenous organic carbon in Arctic Ocean sediments. Organic Geochemistry, 42, 1109-1146.

Wagner, A., Lohmann, G., Prange, M. 2011. Arctic river discharge trends since 7ka BP. Global and Planetary Change, 79 (1) 48-60.

Walsh, F.B. 2006. The Kopanoar mud volcano on the Mackenzie Shelf, Beaufort Sea: implications for methane release on arctic shelves. Atlantic Geology, 42, 120-121.

Walsh, J.E., Fetterer, F., Scott Stewart, J., Chapman, W.L. 2017. A database for depicting Arctic sea ice variations back to 1850. Geographical Review, 107(1), 89-107.

Wang, Z., Chen, J., Yang, P., Qiao, X., Tian, F. 2007. Polycyclic aromatic hydrocarbons in Dalian soils: distribution and toxicity assessment. Journal of Environmental Monitoring, 9, 199-204.

Wang, R., Shu T., Wang B., Yu Y., Chang L., Zhang Y.X., Jing H., Ma J.M., Hung, H. 2010. Sources and pathways of polycyclic aromatic hydrocarbons transported to alert, the Canadian High Arctic. Environmental Science and Technology, 44, 1017-1022.

Weichenthal, S., Van Rikswijk, D., Kulka, R., You, H., Van Ryswyk, K., Willey, J., Dugandzic, R., Sutcliffe, R., Moulton, J., Baike, M., White, L., Charland, J.-P., Jessiman, B. 2015. The impact of a landfill fire on ambient air quality in the north: A case study in Iqaluit, Canada. Environmental Research, 142, 46-50.

Wildland Fire Management and Working Group. 2013. Evaluating past, current and future forest fire loads in Canada. Canadian Council of Forests Ministers, [PDF]: https://www.ccfm.org/pdf/2%20Fire%20Load%20Trends.pdf

Zaborska, A., Carroll, J., Pazdro K., Pempkowiak, J. 2011. Spatio-temporal patterns of PAHs, PCBs and HCB in sediments of the western Barents Sea. Oceanologia, 53, 1005-1026.

Zhao, W., Wang., W., Liu, Y., Dong, L., Jiao, L., Hu, L., Fan, D. 2016. Distribution and sources of polycyclic aromatic hydrocarbons in surface sediments from the Bering Sea and western Arctic Ocean. Marine Pollution Bulletin, 104, 379-3